Noname manuscript No.
(will be inserted by the editor)

On the Impact of White-box Deployment Strategies for Edge AI on Latency and Model Performance

Jaskirat Singh · Bram Adams · Ahmed E. Hassan

Received: date / Accepted: date

Abstract *Context:* Reducing the run-time latency of Machine Learning (ML)-based applications, while ensuring their inference accuracy, is the crucial task of MLOps engineers. To help them achieve this task, Edge AI technologies have been proposed that allow to transform and distribute (parts of) models across mobile, edge, and cloud tiers. To perform such transformations, MLOps engineers have to select and apply one or more operators. Despite the wide range of operators, broadly categorized into white-box (training-based) and black-box (non-training-based) techniques, deciding which type of operator to use in an Edge AI setup to achieve performance advantage is mostly left to the personal judgment of the engineers. *Objective:* In order to help MLOps engineers decide which operator to use in which deployment scenario, this study aims to empirically assess the accuracy vs latency trade-off of white-box and black-box operators (and their combinations) in an Edge AI setup. *Method:* We perform inference experiments including 3 white-box (i.e., QAT, Pruning, Knowledge Distillation), 2 black-box (i.e., Partition, SPTQ) and their combined operators (i.e., Distilled SPTQ, SPTQ Partition) across 3 tiers (i.e., Mobile, Edge, Cloud) on 4 commonly-used Computer Vision and Natural Language Processing models to identify the effective strategies, considering the perspective of MLOps Engineers. *Results:* Our Results indicate that the combination of Distillation and SPTQ operators (i.e., DSPTQ) should be preferred over non-hybrid operators when lower latency is required in the edge at small to medium accuracy drop. Among the non-hybrid operators, the Distilled operator is a better alternative in both mobile and edge tiers for lower latency performance at the cost of small to medium accuracy loss. Moreover, the operators involving distillation show lower latency in resource-constrained tiers (Mobile, Edge) in comparison to the operators involving Partitioning across Mobile and Edge tiers. For textual subject models, which have low input data size requirements, the Cloud tier is a better alternative for the deployment of operators in comparison to the Mobile, Edge, or Mobile-Edge tier (the latter being used for operators involving partitioning). In contrast, for image-based subject models, which have high input data size requirements, the Edge tier is a better alternative for operators in comparison to Mobile, Edge, or their combination.

Keywords Edge AI · White-Box Operators · Black-Box Operators · Deployment Strategies · Latency · Accuracy

Jaskirat Singh
Queen's University
E-mail: 21js160@queensu.ca

Bram Adams
Queen's University
E-mail: bram.adams@queensu.ca

Ahmed E. Hassan
Queen's University
E-mail: hassan@queensu.ca

1 Introduction

In the context of deploying machine learning (ML) models in the context of software products, optimizing model inference latency and performance accuracy is crucial. Ensuring the right trade-off between latency and accuracy is the responsibility of MLOps Engineers, who need to ensure that models deliver reliable predictions consistently, even under varying network conditions and input scenarios. By optimizing model inference, MLOps engineers can minimize the strain on the hardware resources, maximizing the performance of deployed models while minimizing infrastructure costs. Furthermore, optimized model inference contributes to overall system performance and scalability. By striking the right balance between latency and accuracy, and leveraging efficient optimization techniques, MLOps engineers can maximize deployed models' reliability, scalability, and resource utilization, ultimately delivering a seamless and responsive user experience.

Edge AI, or Edge Artificial Intelligence, has emerged as a promising solution for addressing the challenges associated with deploying machine learning model-based applications by bringing computation closer to the data source, thereby enabling faster processing and response times in resource-constrained environments such as Mobile/IoT devices, or edge servers [134]. Edge AI minimizes the latency associated with sending data to centralized cloud servers for processing by performing computation locally on mobile/edge devices. Moreover, this enhances privacy and security by processing data locally on resource-contained devices (i.e., Mobile, Edge), reducing the need to transmit sensitive information to external servers. This mitigates the risk of data breaches or unauthorized access during data transmission, particularly important for applications handling sensitive or confidential data.

The model deployment in the Edge AI environment of Mobile, Edge, and Cloud (MEC) tiers relies on operators, which, according to a prior survey [134] can be divided into white-box operators (training-based) and black-box operators (non-training-based). The black-box operators involve techniques where an already trained model is optimized at the post-training stage. The white-box operators involve techniques where the model is optimized or tailored by exploiting the internal architecture of models using additional training pipelines. By understanding and exploiting the internals of the model using white box operators, the MLOps engineers can apply optimizations that are tailored to the specific characteristics and requirements of the deployment environment, leading to more efficient models in terms of both computational resources and memory footprint. The black-box operators often involve runtime optimizations such as model partitioning, where different parts of the model are executed on different tiers of the Edge AI setup (e.g., some computations are offloaded to the Edge or Cloud tier). Another type of black-box operator is Post Training Quantization, where the pre-trained models are quantized using calibration data. Black-box operators provide more flexibility and may preserve accuracy without modifying the model structure (such as Partitioning) but may not achieve the same level of efficiency as white-box optimizations (such as Knowledge Distillation).

The white-box operators include techniques such as Model Pruning, Quantization-Aware Training (QAT), or architecture optimization. QAT allows the augmentation of the model's computational graph (i.e., allows to modify the model's structure during training) for simulating the effects of quantization. Pruning allows for eliminating unnecessary parameters or nodes/edges, such as weights and connections while maintaining or even improving its accuracy performance. This can be done physically (removing the actual connections) or logically (assigning zero weights to irrelevant connections). While the QAT and Pruning operators accelerate the inference at minimal accuracy loss, architecture optimization such as Knowledge Distillation (KD) involves designing or selecting model architectures that are lightweight and efficient in terms of computational requirements while trying to maintain acceptable performance. White-box operators offer fine-grained control over model optimizations and can lead to significant improvements in latency and efficiency but may require additional time and effort during the training phase. Despite the wide range of black-box and white-box operators, thus far, in the specific setting of Edge AI, only the impact of black-box operators on latency and accuracy has been investigated [108], while studies comparing white-box operators do not consider all three tiers (MEC) of Edge AI for latency and accuracy evaluation.

Hence, the main contribution of this paper is the empirical comparison in terms of latency and accuracy of competing White-box and Black-box operators and their combinations to suggest recommendations for the model deployment for MLOps engineers. Particularly, we study 3 white-box (i.e., QAT, Pruning, Distillation), 2 black-box (i.e., SPTQ, Partition), and their hybrids (i.e., Distilled SPTQ, SPTQ Partition) in an Edge AI environment of MEC (Mobile, Edge, Cloud) tiers. The comparative

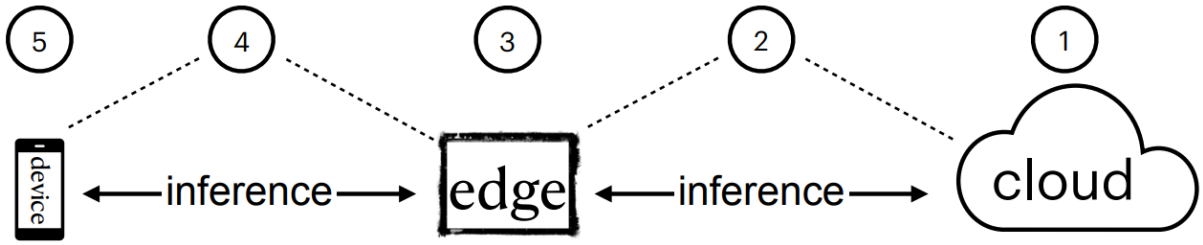

Fig. 1: A visual summary of Single-tier (1,3,5) and Multi-tier (2,4) Edge AI Deployment Strategies

analysis of the mentioned operators w.r.t latency and accuracy performed in our study allows MLOps Engineers to make informed decisions about which optimization techniques to employ based on the specific requirements and constraints of the deployment environment. We explore the following RQs:

- RQ1: What is the impact of QAT-based white box operator on latency and accuracy?
- RQ2: What is the impact of the Pruning-based white box operator on latency and accuracy?
- RQ3: What is the impact of the Knowledge Distillation-based white box operator on latency and accuracy?
- RQ4: What is the impact of the hybrids of white-box and/or black-box operators on latency and accuracy?

The rest of this paper is structured as follows. Section 2 reviews existing literature in the field. Section 3 outlines the methodology, including details on the subject models, experimental setup, performance evaluation metrics, motivation and approach for each research question, and data analysis. Section 4 presents the findings for the four research questions. Section 5 interprets the results and compares the outcomes of the research questions. Section 6 identifies potential threats to the validity of the study, followed by the conclusion in Section 7.

2 Related Work

In earlier investigations [134,118,17,83], various families of deployment operators were explored. Our current study focuses on operators involving model optimization, specifically evaluating three white box operators (QAT, Distillation, and Pruning), two black box operators (SPTQ, Partition), and their combinations (SPTQ Partition, Distilled SPTQ). We aim to provide practical insights derived from empirical data, shedding light on effective strategies for optimizing models to meet the challenges inherent in Edge AI environments, such as constrained computational resources and network limitations. As shown in Table 1, numerous studies emphasize detailed analyses of individual operators or comparisons between them. Only one study [82] compares three operators (white-box), but not in an Edge AI setup, indicating that there is a lack of research comparing a broader set of operators (white-box) in the context of Edge AI to achieve a more thorough analysis of their relative performances and trade-offs, which is the primary goal of our study.

Table 1 shows the distinctive features of our study compared to 25 and 29 prior studies focusing on the white-box Knowledge Distillation and Pruning operator, respectively in isolation or combination with other operators. Out of the 33 studies that focused solely on quantization, 16 utilized a black-box approach, while 17 employed a white-box approach, both of which are also compared in our study. Regarding input data, a greater number of studies focus on image (79) or textual (11)-based models, in comparison to speech models (6), indicating that image/text data is more frequently utilized for the specified operators.

In Table 1, no study considers all 3 Edge AI tiers for white box operators in their experiments, indicating that this aspect of the study is comparatively less investigated. The combination of all 3 tiers offers a more comprehensive perspective on real-time deployment scenarios, encompassing diverse computational and network conditions. Hence, we incorporated all 3 tiers to ensure our Edge AI setup is detailed and adaptable. One previous study [5] in Table 1 employs a simulated Edge AI Setup instead of real hardware, suggesting that such a configuration is viable for evaluating the operators' performance. Moreover, the simulated environment is more economical and handy than physical hardware, while

Table 1: Distinctive Features: Prior Work vs. Our Approach

Ref.	D	PR	Q	O	W	H	SS	M	E	C	LA	ID	TD	SD	RI	AA	CO
Our work	✓X	✓	✓X	P,QP	✓	✓	✓	✓	✓	✓	S	✓	✓		✓	✓	✓
[44]	✓				✓							✓		✓		✓	
[112]	✓				✓							✓				✓	
[102, 2]	✓				✓	✓			✓			✓				✓	
[101]	✓				✓				✓			✓				✓	
[109]	✓				✓				✓		N		✓		N	✓	
[4]	✓			P	✓			✓		✓		✓				✓	
[77, 78, 73, 75]	✓			P	✓	✓		✓	✓		S	✓				✓	
[100]	✓			P	✓	✓			✓	✓		✓				✓	
[74]	✓			P	✓	✓		✓	✓		A	✓			✓	✓	
[92, 65]	✓			E	✓	✓						✓				✓	
[69]	✓			E	✓	✓							✓			✓	
[76]	✓			P,E	✓	✓		✓	✓		S	✓				✓	
[1]	L	L			✓	✓						✓				✓	
[56]	X		✓X		✓	✓						✓				✓	✓
[106]	X		✓X		✓							✓				✓	✓
[54]	X		✓X		✓	✓							✓			✓	✓
[9]	X		✓X		✓	✓						✓	✓			✓	✓
[55]	I	I	✓I		✓	✓						✓				✓	✓
[57]	I	I	I		✓	✓						✓		✓		✓	
[40, 122]		✓			✓	✓						✓				✓	
[124, 12]		✓			✓							✓				✓	
[11]		✓			✓	✓			✓			✓				✓	
[64]		✓			✓				✓		A	✓			✓	✓	
[8]		✓			✓	✓		✓			S	✓		✓	✓	✓	
[27]		✓			✓	✓		✓			A	✓			✓	✓	
[52]		✓			✓				✓			✓				✓	
[68]		✓			✓			✓			N	✓		✓	✓	✓	
[51]		✓		P	✓	✓		✓	✓			✓				✓	
[121]		✓		P	✓	✓		✓			S	✓	✓	✓	✓	✓	
[89]		✓		E	✓	✓					S	✓			✓	✓	
[48]		✓	✓		✓	✓						✓				✓	✓
[42]		✓	✓			✓						✓				✓	✓
[41]		✓V	✓V		✓							✓				✓	✓
[39]		✓V	✓V		✓	✓		✓			S	✓			✓	✓	✓
[116]		✓V	✓V		✓	✓						✓				✓	✓
[46]		✓V	✓V		✓	✓						✓				✓	✓
[123, 113]		✓V	✓V		✓							✓				✓	✓
[97]		V	V		✓							✓	✓			✓	
[107]		V	V		✓	✓						✓				✓	
[38]		V	V		✓	✓					A/S			✓	✓	✓	
[59]		✓V	✓V		✓	✓						✓	✓			✓	✓
[6, 10, 14, 28, 30, 67, 85]			✓									✓				✓	
[60, 79, 86]			✓			✓						✓				✓	
[31, 47, 130]			✓			✓						✓	✓			✓	
[66]			✓			✓					N	✓			✓	✓	
[93, 132]			✓		✓	✓			✓			✓				✓	
[22, 13, 35, 133, 71]			✓		✓	✓						✓				✓	
[25, 50, 115, 87]			✓		✓	✓						✓				✓	
[7]			✓		✓							✓				✓	
[26, 105, 99]			✓		✓	✓						✓	✓			✓	
[49]			✓		✓	✓		✓			N	✓			N	✓	
[111]			✓		✓						A	✓			✓	✓	
[63]			✓	P					✓	✓	S	✓				✓	
[5]			✓	P		✓	✓		✓	✓	S	✓				✓	
[82]	✓XIL	✓VIL	✓XVI		✓								✓			✓	✓

[1] D: Distillation, PR: Pruning, Q: Quantization, X: Combination of Distillation and Quantization, V: Combination of Pruning and Quantization, L: Distillation + Pruning, I: Distillation + Pruning + Quantization, O: Additional Operators (P: Partitioning, QP: Quantized (SPTQ) Partitioning, E: Early Exiting), W: White-Box Transformations, H: Hyper-parameters (Non-empty cells indicate default hyper-parameters, while an empty cell represents hyper-parameter tuning or analysis), SS: Simulated Setup (empty cell represents Real or Emulated Hardware Setup), MEC: Mobile Edge Cloud, LA: Latency Approach (S: Sequential, A: Asynchronous, N: Unmentioned), ID: Image Data, TD: Textual Data, SD: Speech Data, RI: Range of Input Sizes (for latency experiment), AA: Analysis of Accuracy, CO: Comparison across Operators, Empty cells of MEC highlight that they are not an Edge AI setup

ensuring a controlled setting, simplifying the isolation and micro-bench marking of latency performance for individual operators. There are four other studies [125,84,21,81] also considered simulated Edge AI setup for black box operator (Partitioning). Conversely, although simulations can closely mimic the operation of actual hardware, they might not reproduce all the intricacies of a real-world setting including hardware/network variations, power usage, and real-time limitations. Regarding MEC tiers, Inference Latency Approach, and Range of Inputs, there is no investigation into the sequential inference of a variety of inputs (with different sizes) within an edge AI environment of MEC tiers for white box operators, which was explored in our study.

In studies examining interconnected multi-tier networks, the majority (7 out of 8) focus on Sequential Inference for latency assessment across the tiers, as opposed to Asynchronous Inference (1 out of 8). In sequential inference, tasks progress step by step across the network tiers and rely on each other, with each task waiting for the previous one to finish. Conversely, asynchronous inference involves tasks across tiers being performed concurrently or independently. We opted for sequential inference to isolate the performance characteristics of individual operators in a controlled setting. This approach allows for a more deterministic assessment of the impact of input data sizes and network/computational resources of heterogeneous MEC tiers on the operator's latency, akin to micro-benchmarks.

We concentrate on operators associated with model transformations, i.e., alterations in ML models' structure, parameters, or behavior. These operators can be divided into two categories: white-box and black-box. Previous research has examined white-box operators such as Pruning and Distillation, and a black-box operator known as Model Partitioning. Some operators, like Quantization, can be implemented in both black box (SPTQ) and white box (QAT) modes. We conducted a thorough study of the white box (Knowledge Distillation, Pruning, QAT), black box (Partition, SPTQ Partition), and their hybrids (Distilled SPTQ), aiming to address empirical insights into optimizing models effectively and addressing the issues encountered during deployment in diverse Edge AI setup.

In conclusion, our research presents a novel empirical investigation into Edge AI Deployment Strategies. These strategies involve mapping white-box, black-box, and their hybrid operators onto Edge AI tiers to assess the best trade-off of latency vs accuracy. To the best of our understanding, previous research (Table 1) lacks a detailed study on the comparative analysis of three white-box (Knowledge Distillation, Pruning, QAT) and two black-box (i.e., SPTQ, Partitioning) operators, along with their hybrids (Distilled SPTQ, SPTQ Partitioning) in the setting of Edge AI. Furthermore, unlike previous studies (Table 1), our research evaluates the round trip (end-to-end) latency of operators in an Edge AI environment. Lastly, our emphasis is on measuring the latency across various input (i.e., image) sizes using sequential inference requests, a factor not explored in prior studies. This aspect aids in analyzing the influence of input data on the presented deployment operators.

2.1 Knowledge Distillation

Knowledge distillation [44,112,102,2,101,109,4,77,78,73,75,100,74,92,65,69,76,1,56,106,54,9,55,57,82] is a family of Edge AI deployment operators that aims to transfer knowledge from a large, complex model (the teacher) to a smaller, simpler model (the student) [33]. This process involves training the teacher model on a task, generating soft targets (probability distributions) using the teacher's predictions, then training the student model to replicate these soft targets while also using the original labeled data. The primary goal of knowledge distillation is to improve the performance of the smaller model while reducing its computational and memory requirements. As smaller models are less expensive to evaluate, they can be deployed on less powerful hardware (such as a mobile device). The teacher model typically has higher accuracy but may be computationally expensive for deployment in resource-constrained environments, such as mobile or edge devices. By distilling the knowledge from the teacher model into the student model, the aim is to create a more efficient and lightweight model that retains much of the performance of the teacher model.

2.2 QAT

Quantization Aware Training (QAT) [93,132,22,35,133,13,71,25,50,7,115,87,26,105,99,49,111,41,116, 123,59,82,56,106,54,9,55,57] is a family of Edge AI deployment operators that involves quantization

of all model weights/activations in the forward/backward training passes to simulate the quantization process. This is done by inserting "fake quantize" nodes at appropriate places in the model. These nodes mimic the effect of quantization (reducing the precision of weights/activations) during the forward pass of the model but allow gradients to pass through during the backward pass. These operations round the values to the target precision but do not change the data type or numerical representation. After training, the model is converted to use lower-precision weights and activations, which involves replacing the fake quantization operations with actual quantization operations. QAT usually yields higher accuracy than the post-training static quantization but at a computational cost of re-training the model [32].

2.3 Pruning

Pruning involves "pruning" certain weights (making them zero) that are deemed less critical for the model's performance. A pruned model with zero weights can result in faster computations during inference as the zero weights allow for more efficient matrix operations, reducing the number of multiplications and additions. In particular, it involves identifying and removing unnecessary connections, weights, or neurons from a trained deep learning model, resulting in a more compact model that is easier to deploy and consumes less memory and hardware resources. The primary objective of model pruning is to make models more computationally efficient, reduce memory requirements, and, in some cases, improve the model's inference speed.

There are two kinds of pruning, i.e., physical and logical pruning, as explained below:

- Physical Pruning: In physical pruning, the connections that received a zero weight are removed from the model. This means that these weights are no longer stored, and the computations involving these weights are skipped, resulting in a smaller and faster model. This is particularly useful for deploying models on resource-constrained devices, where storage and computational resources are limited. [40, 124, 122, 12, 11, 64, 8, 27, 52, 68, 51, 121, 89, 48, 41, 39, 116, 46, 123, 113, 97, 38, 59, 55, 57, 1, 82]
- Logical Pruning: In logical pruning, the connections to be pruned are not physically removed from the model. Instead, they are masked or set to zero but still stored in the model. During inference, masked weights are multiplied by zero, effectively excluding them from computations. [126, 104]

3 Methodology

This section elaborates on the methodology adopted to tackle the research questions outlined in the introduction.

3.1 Subject Models

We opted for diverse models to maintain representativeness in our experiment, focusing on Computer Vision and NLP tasks. Our subject models were chosen from the PyTorch ImageNet Models store[1] and Hugging Face store [2] to ensure a range of architectures, sizes, and scopes. To capture realistic scenarios, we selected models with varying complexities for both image and text classification tasks, as outlined in Table 2. These models were selected because of their popularity in research (Table1 1) and their compatibility with the Intel Neural Compressor (INC) tool used for the generation of white box operators. In recent studies [103, 36, 104], INC is commonly used for optimizing trained Deep Learning (DL) models and it provides popular model compression techniques such as low-precision quantization, pruning, knowledge distillation, and other compression techniques.

Image classification is an ML task that aims to set a label/category to an input image. This process involves training a model using a labeled image dataset and then utilizing this trained model to predict labels for new, unseen images [72]. Likewise, text classification entails assigning predetermined categories or labels to textual documents or pieces of text, which is accomplished by training a model on a dataset containing labeled texts.

[1] https://pytorch.org/vision/main/models.html
[2] https://huggingface.co/

For image classification models (ResNet and ResNext), we employed the Image-Net dataset, a well-established benchmark in the field. For text classification models (Bert and Roberta), we utilized the MRPC (Microsoft Research Paraphrase Corpus) dataset, suitable for evaluating performance metrics in NLP tasks.

Table 2: Subject models

Model Name	**Model Size**	**Parameters**	**Scope**	**Dataset**
ResNet [127]	484MB	126.81M	Image Classification	ILSVRC 2012 [98]
ResNext [120]	319MB	83.35M	Image Classification	ILSVRC 2012 [98]
Bert [18]	438MB	109.48M	Text Classification	MRPC [20]
Roberta [70]	499MB	124.64M	Text Classification	MRPC [20]

3.2 Study Design

We examine the trade-off between two measurable factors: latency and accuracy. This evaluation is pivotal for grasping how accuracy and latency perform in an Edge AI setup, offering insights into optimal strategy selection tailored to deployment engineers' specific needs and scenarios. Some scenarios may prioritize minimizing latency, potentially compromising accuracy, while others may prioritize accuracy despite a slight increase in latency. Our empirical findings, derived from deploying diverse operators on distinct tiers, establish a quantitative framework for assessing this trade-off. Additionally, it forms the basis for our long-term objective (beyond this paper's scope): developing recommendation systems that can automatically suggest the most suitable operators and deployment strategies based on specific requirements for latency and accuracy.

From the broader set of 8 operator families for Edge AI Inference, as outlined in Section 1, we narrow our focus in this study to investigate operators specifically tailored for optimizing models in a white box manner. This entails re-training models on the training data for the white-box operators. Among the available white box operators, we have chosen three of them based on their diverse approaches and feasibility: Quantization Aware Training (QAT), Model Pruning, and Knowledge Distillation. These operators are quite popular in research as shown in Table 1. These operators were selected for their capacity to address various aspects of model optimization, including enhancing inference speed and preserving performance.

QAT was selected as it minimizes the impact of quantization on model accuracy by training the model with awareness of the quantization process. This can be advantageous in scenarios where maintaining model performance is crucial. It explicitly considers the effects of quantization during training, potentially resulting in models that are more robust to the quantization process. Pruning identifies connections or weights that contribute less to the overall model performance and prunes them by setting the connections' weight values to zero (logical pruning) or removing those zero-weight connections (physical pruning) to create a more sparse model, which can lead to faster computations during inference. The motivation for considering Knowledge Distillation as an operator is its aim to compress the knowledge of the teacher model into a more compact student model that is easier to deploy and requires fewer computational resources. This would especially be valuable in scenarios where resources are constrained (i.e., mobile and edge tiers).

The performance and latency of QAT, Pruned, and Distilled models are compared with the original models and with each other to analyze their robustness in the Edge AI Environment. We compared these 3 white box operators with a family of black box operators such as Partitioning and SPTQ from a previous study [108]. Additionally, combinations of black box operators (SPTQ + Partitioning) and white/black box operators (Knowledge Distillation + SPTQ) are performed to collect empirical data to analyze how these hybrid operators perform under real-world scenarios. From the black-box operators studied in our prior work [108] and the white-box operators studied in this paper, we excluded the hybrids involving pruning due to the incompatibility of pruning to provide a performance advantage in our study, and we also excluded the Early Exiting operator due to its in-feasibility for textual subject models and

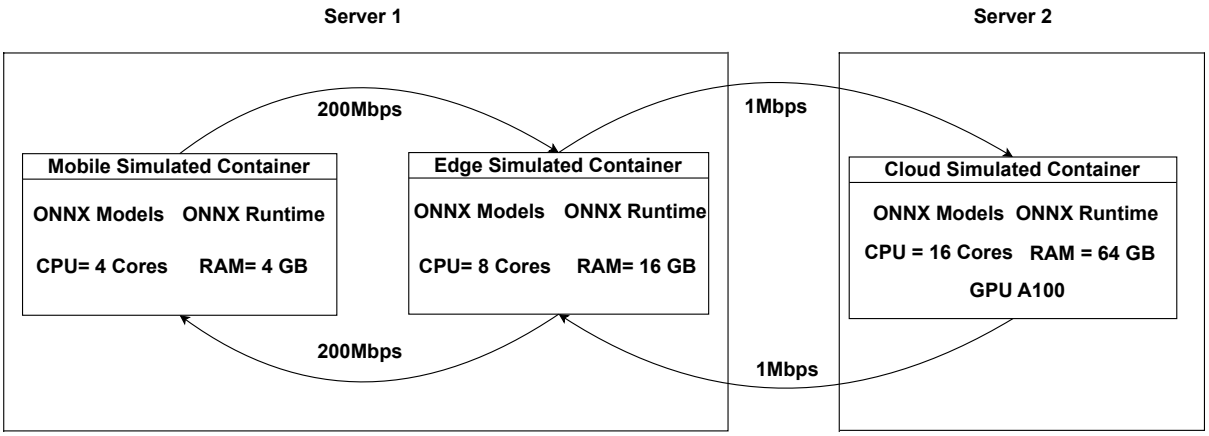

Fig. 2: Graphical illustration of Experimental Architecture for Edge AI

its lower accuracy/latency benefits. The intricate architecture of the ONNX computational graphs for textual models involves numerous layers, connections, and branching structures. This complexity poses challenges in identifying viable early exit points for this operator, requiring extensive manual analysis and modifications to the model's computational graph. Such a process could be time-consuming and error-prone due to the intricate nature of textual model architectures. Moreover, the Early Exiting operator [108] is more sensitive to accuracy performance degradation in comparison to other operators like Quantization and Partitioning. In terms of latency, the Early Exiting operator was not better than the Quantized models during Edge deployment. We excluded the hybrids involving pruning due to their ineffectiveness in providing latency and performance benefits in our study.

In our study, we used the training pipelines from the INC tool for the white box operators (i.e., QAT, Pruning, and Distillation). The choice of this tool is based on its readily available pipelines for the white box operators through well-designed APIs for a wide range of models (textual and image models). By providing APIs for various DL frameworks (TensorFlow, PyTorch, MXNet, ONNX runtime), INC ensures that model compression techniques can be applied consistently across them. This interoperability of INC allows researchers and practitioners to use their preferred framework while benefiting from efficient model deployment. There is no other similar tool that provides the specialized implementation for various kinds of white-box operators across DL frameworks. Moreover, the INC tool is quite a popular state-of-the-art tool used in collaboration with cloud platforms (Google Cloud [3], Alibaba Cloud [4]), software platforms (Microsoft Olive [5], Tencent TACO [6]), and open AI ecosystems (ONNX [7], Hugging Face [8]) for model optimization. We monitored the training time of the white box operators to understand the time complexity of generating these operators in real-world scenarios.

3.3 Experimental Setup

We created a simulation of an Edge AI deployment framework encompassing mobile, edge, and cloud tiers, as illustrated in Figure 2. Notably, we utilized Docker containers, inspired by previous studies [95, 94], to simulate the hardware and network setups of real mobile, edge, and cloud environments. Docker, a widely used open-source containerization technology [80], provides a consistent and easily portable environment, a lightweight, portable container that includes all necessary dependencies, libraries, and configurations for

[3] https://networkbuilders.intel.com/solutionslibrary/intel-deep-learning-boost-boost-network-security-ai-inference-performance-in-google-cloud-platform-gcp-technology-guide

[4] https://medium.com/intel-analytics-software/alibaba-cloud-collaborates-with-intel-neural-compressor-for-better-productivity-and-performance-83cdb6500420

[5] https://cloudblogs.microsoft.com/opensource/2023/06/26/automate-optimization-techniques-for-transformer-models

[6] https://mp.weixin.qq.com/s/CPz9-5Nsh-5N9Q8-UmK–w

[7] https://community.intel.com/t5/Blogs/Tech-Innovation/Artificial-Intelligence-AI/Quantizing-ONNX-Models-using-Intel-Neural-Compressor/post/1355237

[8] https://huggingface.co/blog/intel

running a software application. It offers a standardized and portable format for packaging and distributing applications, compatible with various platforms, including cloud, on-premise, and edge.

In our Edge AI setup, there are two servers involved, i.e., one with the cloud container and one with the mobile/edge container. To contend with the diverse nature of resource-constrained mobile and edge tiers, we deployed the ONNX Run-time Executor with the CPU Execution Provider in resource-aware Docker containers on one server containing both mobile and edge tiers. The configurations of these containers mirrored real-world scenarios, featuring quad-core and octa-core CPUs (Intel(R) Xeon(R) E7-4870 2.40GHz), along with 4GB and 16GB RAM for mobile and edge tiers, respectively based on previous studies [23, 19]. This choice reflects the practical constraints often seen in edge devices, where dedicated GPUs may be absent due to power, size, or cost limitations. The Docker container representing the cloud was configured on a distinct server, equipped with 16-core CPUs (Intel(R) Xeon(R) Platinum 8268 CPU 2.90GHz), 64GB RAM, and an NVIDIA A100 GPU. This configuration is based on previous studies [58, 96]. The cloud executed all inference experiments on its GPU using ONNX Run-time with the CUDA Execution Provider.

Interconnected via a common network bridge in Docker, the simulated mobile and edge containers communicate with each other via API requests. Additionally, the edge container establishes a connection with the external simulated cloud container. The Linux Traffic Control utility[9] configured within each Docker container facilitates the simulation of mobile-edge and edge-cloud network bandwidths. After generating white box, black box, and hybrid operators, resulting .onnx files were deployed on the corresponding simulated devices. The Flask Framework managed incoming and outgoing requests seamlessly across mobile, edge, and cloud devices. Employing Base64 encoding during data transfer ensured reliable and universally readable data transmission. For both image and textual models, the final output transmitted across the Edge AI Environment comprised of predicted labels, which have smaller sizes than the network bandwidths of the Edge AI Environment.

Drawing on the earlier work [88, 129, 110, 29, 3], we set an edge-cloud bandwidth of 1 Mbps to simulate Wide Area Network (WAN) transmission latency and a mobile-edge bandwidth of 200 Mbps was selected to represent Wireless Local Area Network (WLAN) transmission latency. These bandwidth choices aimed to capture the typical network conditions observed in WAN and WLAN environments. WAN connections, frequently employed for communication between edge and cloud over expansive geographical distances, often feature lower bandwidth due to factors like network congestion and long-distance transmission. In contrast, WLAN connections, localized and commonly used for mobile and edge device connectivity, tend to offer higher bandwidth.

To mitigate the computational expense and time constraints associated with the entire validation dataset of Image and Textual subject models for inference experiments, we strategically conducted experiments on a representative subset of 100 samples. Specifically selected from the validation sets of ILSVRC and MRPC (Table 2), these samples featured larger sizes compared to the remaining set, presenting computational challenges stemming from increased memory requirements and processing complexity. This subset approach allowed us to assess an upper bound for inference latency performance and scalability in the context of resource and network constraints. While the subset approach provides practical benefits, it inherently introduces potential bias. Adhering to the recommended minimum sample size of 100 ensured statistical reliability and the derivation of meaningful conclusions [34].

The accuracy assessment of the operators (Identity, SPTQ, QAT, Pruning, Distillation, Distilled SPTQ) is computed independently. This evaluation takes place within CPU-based Docker environments (i.e., mobile, edge) and GPU-based Docker environments (i.e., cloud). The rationale behind this approach is to gauge the impact of underlying hardware on the operators' performance. By conducting accuracy assessments across mobile, edge, and cloud Docker containers, we aim for a comprehensive understanding of the model's generalizability across different hardware platforms. The performance of QAT models for textual subject models is reported in the PyTorch framework due to performance issues in the ONNX framework, as certain PyTorch-specific quantization operations were not fully supported in the ONNX format.

The inference experiments comprise two stages: a trial inference experiment and a final inference experiment. For each deployment strategy, a trial inference experiment encompassing 100 sequential runs (i.e., inference of 100 different input test samples as mentioned earlier) served as a cache warm-up phase. This phase aimed to ensure that the cache memory remained in a steady state before initiating

[9] https://man7.org/linux/man-pages/man8/tc.8.html

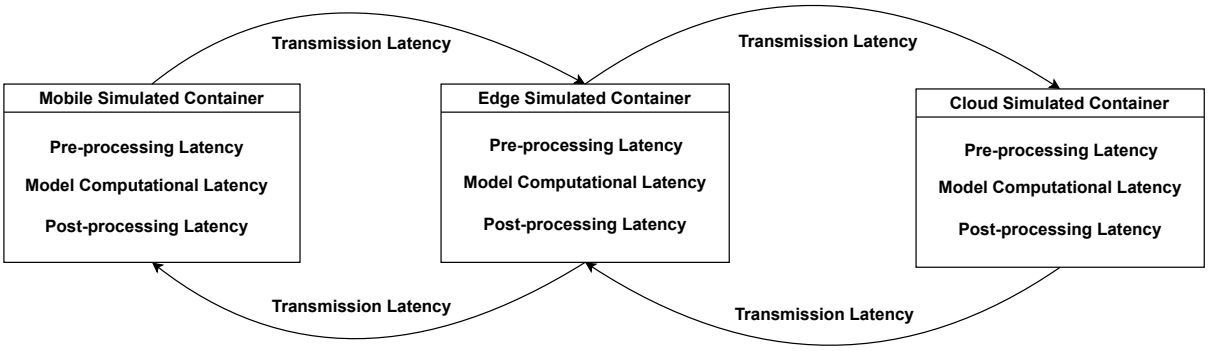

Fig. 3: Graphical illustration of different types of latency contributing to the overall Inference Latency in our experimental setup of 3 containers.

the final inference experiment on the same samples. The cache warm-up phase sought to emulate real-world deployment scenarios where the model is continuously utilized, gradually populating the cache with frequently accessed data, as opposed to performing inference from a cold start. Subsequently, the final inference experiment comprised 500 sequential runs, resulting from the same 100 input test samples executed five times (5 repetitions). The incorporation of multiple repetitions aimed to enhance statistical significance, capture variability, and account for potential performance fluctuations during real-world repetitive inference tasks. The inference latency (in seconds) for each run in the final inference experiment was logged in a .txt file. Following the completion of each final inference experiment of 500 sequential runs, the simulated mobile, edge, and/or cloud Docker containers underwent a restart, ensuring that subsequent experiments occurred in a consistent and isolated environment, thereby fostering more reliable and reproducible results.

Within the scope of our study, deployment strategies manifested as a mapping of deployment tiers to one or more deployment operators. These deployment tiers denote the physical locations for model deployments, encompassing three single-tier environments (i.e., mobile, edge, and cloud) and one multi-tier environment (i.e., mobile-edge). Single tiers involve deploying entire models on individual computing tiers to achieve monolithic inference, while multi-tiers encompass the deployment of partitioned models across multiple computing tiers to facilitate distributed inference. Deployment operators constitute white-box and black-box operators applied to DL models for efficient deployment and execution within the Edge AI Environment. These operators could be categorized as singular operators, involving individual optimization techniques applied independently, or hybrid operators, combining multiple singular optimization techniques.

3.4 Metrics for evaluating model performance

3.4.1 Inference Latency

The measurement of Inference Latency encompasses the sum of pre-processing latency, model computational latency, post-processing latency, and transmission latency, as mentioned in Figure 3. The pre-processing latency accounts for the time spent adapting input data to meet the model's requirements. Model computational latency involves the duration of the forward pass in a neural network, encompassing input propagation, mathematical operations, and output generation. Post-processing latency reflects the time dedicated to refining and interpreting the model's output after the forward pass. Transmission latency signifies the time taken for data to traverse from one tier to another within an Edge AI network.

For the quantification of Inference Latency, we employ a timer initiated just before the commencement of an inference test run, ceasing upon the model's successful return of output. To achieve this, we utilize the default_timer function from the Python timeit package. Throughout the analysis of the four research questions, the terms "speedup" and "slowdown" are employed to denote the degree by which the median inference latency of a specific operator outpaces or lags behind the median inference latency of another operator. This terminology is instrumental in conveying the comparative latency of different operators.

3.4.2 Accuracy

For distinct domain-specific models, the preferred accuracy metric varies. In our investigation, we use specific metrics, namely Top 1% and Top 5% Accuracy to assess the performance of image classification models such as ResNet and ResNext. For text classification models like Bert and Roberta, we utilize the F1 Score [117, 18, 70] as the accuracy metric. Broadly, we determined accuracy metrics by validating each model on its dedicated validation dataset for a more precise evaluation of their accuracy, as detailed in Table 2. The definitions of these metrics are as follows:

- Top5% and Top1% Accuracy: Top-5 Accuracy gauges the proportion of validation samples where the true label is within the top 5 predictions (in terms of a model's highest confidence scores). On the other hand, Top-1 Accuracy is a stricter metric, indicating the proportion of validation samples where the model's highest confidence prediction precisely matches the true label. Both metrics are valuable in image classification tasks, providing a comprehensive evaluation of the model's effectiveness. Consequently, we utilize both Top-1 and Top-5 accuracy measurements to obtain a thorough understanding of image classification model performance in our study.
- F1 Score: The F1 score is a metric used to evaluate the performance of a classification model, particularly in binary classification tasks. It is the harmonic mean of precision and recall, providing a balance between these two metrics. The reason for using the F1 Score as an evaluation metric for textual classification models is that it is sensitive to both false positives and false negatives.

The image classification models were assessed on the ILSVRC 2012 dataset (50k validation samples), whereas the textual classification models underwent validation on the MRPC dataset (408 validation samples). The term "accuracy" is uniformly used to denote the accuracy metrics across all four subjects in the results of the research questions.

In our analysis, we opted to exclude accuracy evaluations for operators involving partitioning, aligning with findings from prior research [62]. These studies suggest that model partitioning has no discernible impact on inference accuracy, as it essentially transmits the same intermediate results remotely instead of within the same tier. Given the inherent sequential processing nature of the model's architecture, partitioning ensures that data flows through each partitioned model in a manner consistent with the original model's design, thereby preserving accuracy.

3.5 Research Questions

3.5.1 RQ1: What is the impact of QAT-based white box operator on latency and accuracy?

Motivation This research question aims to empirically assess the effectiveness of the QAT in comparison to baseline (SPTQ, Identity) models in terms of latency in the corresponding monolithic tiers (i.e., mobile, edge, and cloud). Moreover, the accuracy of the QAT, SPTQ, and Identity operators is validated in each of the monolithic tiers and compared with each other. The RQ helps understand how different quantization techniques perform in real-world deployment scenarios.

Approach The SPTQ was performed using the Intel Neural Compressor (INC) tool on subject models in ONNX format. As the QAT is not yet supported for ONNX models, we have to first apply QAT to the subject models in the Pytorch format, then export the generated QAT models to the ONNX format for measuring the latency. For QAT image models, we computed the accuracy in ONNX format, but for the QAT textual models, we considered the Pytorch format for accuracy evaluation as the QAT textual models in ONNX format encountered accuracy performance issues possibly due to QAT Operations (i.e., Fake Quantization Operations) not being supported by the ONNX format.

The motivation to consider the ONNX format is based on its feasibility for black-box operators as explained in our previous study [108]. Moreover, ONNX provides a way to migrate models between different frameworks (such as PyTorch), which allows training a model in one framework and then deploying it using another for inference. The textual QAT models were exported using Dynamic Quantization APIs to achieve the same model size as before exportation. We considered CPU instead of GPU for the QAT and SPTQ operators, due to the unsupportability of quantization in the GPUs in our setup specifically. Fixing this requires modifying the existing codebase of INC, ensuring compatibility with GPU-specific libraries,

and thorough testing, which would require significant developer resources and a deep understanding of both CUDA programming and the INC framework. We performed the QAT and SPTQ operators on subject models using the default hyper-parameter values listed in the INC repository [10] [11] [12] [13], similar to previous studies (56 out of 83), as shown in Table 1.

3.5.2 RQ2: What is the impact of the Pruning-based white box operator on latency and accuracy?

Motivation This question aims to empirically compare the inference latency and accuracy performance of the Pruning operator relative to Identity, QAT, and SPTQ operators in each of the monolithic tiers (i.e., mobile, edge, and cloud). This research question will answer whether the pruning operator is worth the effort to perform for latency/accuracy benefits.

Approach For logical pruning of subject models, the hyper-parameters listed in the INC repository [14][15] again were considered. The important parameters for logical pruning are the pruning pattern, the target sparsity, and the pruning type. The pruning pattern defines the rules of pruned weights' arrangements in space. The default N×M Pruning pattern for the subject models (i.e., 4×1 and 2×1 patterns for textual and image models, respectively) was selected. In N×M pruning, N−M weights are selected for pruning from each of the M consecutive weights. Target sparsity refers to the proportion of zero weights in the model while performing logical pruning. For textual and image models, 90% and 75% of sparsity were used, respectively, which implies that 90% and 75% of the weights have been pruned (set to zero).

The pruning type determines how the weights of a neural network are scored and pruned. We considered the default pruning type, i.e., snip momentum, which improves the SNIP algorithm [61] by updating the scores in a momentum way. We performed distributed training with multiple GPUs (8 GPUS) for pruning of image models due to higher training iterations, large training data, and high computational/memory requirements. For the pruning of textual models, a single GPU was enough to provide a faster training time due to lower training iterations, small training data, and lower computational/memory requirements.

In our study, we considered the INC tool for performing pruning, as it provides automated pipelines for a wide range of subject models including both image and textual inference tasks. We considered logical pruning as it is more widely used across a wide range of subject models in the INC tool and currently, INC does not support physical pruning for the NxM sparsity pattern used in our study. Its physical pruning is under development and only supports some particular structures (i.e., transformer models) using the channelx1 pruning pattern in the INC tool. In order to ensure consistent pruning across all four subject models in our study, in this study we stick to NxM logical pruning for fair and consistent analysis.

3.5.3 RQ3:What is the impact of the Knowledge Distillation-based white box operator on latency and accuracy?

Motivation This question aims to empirically assess the latency of the Distilled operator and compare it with the Identity, SPTQ, QAT, and Pruned operators in the corresponding tiers (i.e., mobile, edge, and cloud). The accuracy of the Distilled operator is validated in the monolithic tiers and compared with the Identity, SPTQ, QAT, and pruned operators to assess the performance deviation.

[10] `https://github.com/intel/neural-compressor/tree/master/examples/pytorch/nlp/huggingface_models/text-classification/quantization/qat/fx`

[11] `https://github.com/intel/neural-compressor/tree/master/examples/onnxrt/nlp/huggingface_model/text_classification/quantization/ptq_static`

[12] `https://github.com/intel/neural-compressor/tree/master/examples/pytorch/image_recognition/torchvision_models/quantization/qat/fx`

[13] `https://github.com/intel/neural-compressor/tree/master/examples/onnxrt/image_recognition/resnet50_torchvision/quantization/ptq_static`

[14] `https://github.com/intel/neural-compressor/tree/master/examples/pytorch/image_recognition/ResNet50/pruning/eager`

[15] `https://github.com/intel/neural-compressor/blob/master/examples/pytorch/nlp/huggingface_models/text-classification/pruning/eager/scripts/bertmini_sst2_4x1.sh`

Approach In our study, the distillation process involves replicating the behavior of a teacher model (larger and complex architecture) by training a student model (smaller and simpler architecture) to achieve accuracy comparable to the teacher model. The student model is often designed to have a similar architecture to the teacher model. The Knowledge Distillation was performed using the INC tool from teacher to student model in Pytorch format due to its support for distillation. The generated distilled student models were then exported to ONNX format for measuring the latency and accuracy results. Table 3 shows the size and parameters of the teacher and the student models considered for knowledge distillation. Both the student and parent models contain pretrained weights. These pretrained weights provide the student model with foundational knowledge about the domain and allow quicker convergence during knowledge distillation. This helps in improving the performance during knowledge distillation as the representations learned by both student and teacher models are more likely to be compatible, making it easier for the student model to mimic the teacher's knowledge. Considering that pretrained weights of the student model are quite common in scenarios when their architecture is similar to the parent model, the training hyper-parameters listed in the INC repository [16][17] again were considered. For the distillation of ResNet and ResNext subject models, distributed training with multiple GPUs (i.e., 8 GPUs) again was used. In contrast, for the distillation of Bert and Roberta subject models, a single CPU was enough to provide quick training.

Table 3: Parent and Student Models for Knowledge Distillation

Parent Model Name	Parent Model Size	Parent Model Parameters	Student Model	Student Model Size	Student Model Parameters
Wide ResNet-101-2 [127]	484MB	126.81M	Wide ResNet-50-2 [127]	264MB	68.9M
ResNeXt-101 64x4d [120]	319MB	83.35M	ResNeXt-50 32x4d [120]	96MB	25.0M
Bert [18]	438MB	109.48M	Bert Small [114]	110MB	28.76M
Roberta [70]	499MB	124.64M	Roberta Tiny [114]	107MB	27.98M

3.5.4 RQ4: What is the impact of the hybrid applications of white box and/or black box operators on latency and accuracy?

Motivation This question aims to empirically assess the latency and accuracy of combining the white-box (Distillation) operator with the black-box (SPTQ) operator, due to the latency and/or accuracy advantage of SPTQ and Distillation in RQ1 and RQ3, respectively. In a first dimension, the DSPTQ hybrid operator is compared with non-hybrid operators (i.e., Distilled, SPTQ, QAT, Pruned, Identity) in each of the monolithic tiers in terms of latency and accuracy. In a second dimension, the Mobile-Edge Identity Partitioning (MEIP) strategy is compared with the white box operators, and the DSPTQ hybrid operator is compared with the Mobile-Edge SPTQ Partitioning (MESP) strategy.

Approach For the DSPTQ operator, the distillation process was performed on the subject models in Pytorch format using INC as explained in the RQ3 approach. For textual subject models, the distilled models are exported to ONNX first and then the SPTQ process is performed similarly to the RQ1 SPTQ approach for generating DSPTQ models. However, for image DSTPQ models, their SPTQ process was not effectively reducing all the weights to quantized INT8 precision type in ONNX format, due to which we conducted their SPTQ process in Pytorch format before exporting the generated DSTPQ models to ONNX format for latency and accuracy evaluation.

For the Partitioning of the Identity and SPTQ image-based models, we followed our earlier algorithm [108] for creating equal-size sub-models. This algorithm traverses the ONNX computational graph of models in reverse order (from the end) and heuristically selects the partitioning point, i.e., node connection(s), that splits the model into two nearly equal-sized sub-models, which requires manually checking the sizes of partitioned models. In the context of ONNX graphs, the partitioning point refers to the location in the graph where this division of the graph into smaller sub-graphs (or sub-models) occurs.

[16] `https://github.com/intel/neural-compressor/tree/master/examples/pytorch/nlp/huggingface_models/text-classification/optimization_pipeline/prune_once_for_all/fx`

[17] `https://github.com/intel/neural-compressor/tree/master/examples/pytorch/image_recognition/torchvision_models/distillation/eager`

However, for textual subject models, this algorithm was not feasible due to their complex ONNX graph architectures and therefore, we split these models based on the criteria that the first-half sub-model should have a lower model size compared to the second-half sub-model. This criterion is beneficial as the second-half sub-model will reside in a high-resource edge environment in comparison to the first-half sub-model (which resides in a low-resource mobile environment) during distributed inference across the Mobile-Edge tier in our study. For this criterion, we were able to find only one available partition point for the textual models, resulting in unequal-sized sub-models (47MB to 62MB and 179MB to 237MB size difference of SPTQ and Identity Partitioned textual sub-models, respectively).

The graphical illustrations of the algorithms used for Partitioning are provided in the Appendix (Figure 11 12 13 14 15 16), while we refer to the prior paper for more details [108]. The Mobile-Edge tier is used for the deployment of Identity Partitioning, and SPTQ Partitioning operators based on the latency advantage of the Mobile-Edge tier over other tiers (Edge-Cloud, Mobile-Cloud) [108]. The strategies for these combinations of operators and tiers are denoted as Mobile-Edge Identity Partitioning (MEIP) and Mobile-Edge SPTQ Partitioning (MESP).

Table 4: Design of KW and Conover statistical test results for inference latency comparison of Monolithic Identity/Pruned/QAT/Distilled strategies with MEIP strategy and Monolithic DSPTQ strategies with MESP strategy for RQ4 and Discussion Section.

T \ O	I
M	X
E	X
C	X
ME	X

(a) Identity operator comparison across MEC tiers and with MEIP strategy

T \ O	I	QAT
M		X
E		X
C		X
ME	X	

(b) QAT operator comparison across MEC tiers and with MEIP strategy

T \ O	I	SPTQ
M		X
E		X
C		X
ME	X	

(c) SPTQ operator comparison across MEC tiers and with MEIP strategy

T \ O	I	P
M		X
E		X
C		X
ME	X	

(d) Pruned operator comparison across MEC tiers and with MEIP strategy

T \ O	I	D
M		X
E		X
C		X
ME	X	

(e) Distilled operator comparison across MEC tiers and with MEIP strategy

T \ O	SPTQ	DSPTQ
M		X
E		X
C		X
ME	X	

(f) DSPTQ operator comparison across MEC tiers and with MESP strategy

3.6 Data Analysis

In the analysis of the results from the inference latency experiments, we employed several statistical methods. Initially, we utilized the Shapiro-Wilks test and Q-Q plot for each deployment strategy to evaluate the normality of the inference latency distribution. This helped us decide whether to use parametric or non-parametric tests for hypothesis testing. As the data did not exhibit a normal distribution, we proceeded to use the Kruskal-Wallis (KW) test [91]. This test allowed us to compare the inference latency distributions among 3 or more independent groups, representing different deployment strategies. If the KW test states a significant difference, we further employ the Conover post-hoc test [16] to perform pairwise comparisons. We focused on two dimensions, namely operator and tier, to determine if a significant difference existed among at least two independent groups through hypothesis testing. The design approach for the KW and Conover statistical tests across the tier and operator dimensions is detailed in Table 4 and Table 5, respectively.

When conducting the Shapiro-Wilks, Kruskal-Wallis, and Posthoc Conover tests, we assess the obtained p-value against a significance level of alpha = 0.05 by default. The interpretation of Cliff's delta effect sizes [15] [43], categorizes them as negligible ($d < 0.147$), small ($0.147 \leq d < 0.33$), medium ($0.33 \leq d < 0.474$), or large ($d \geq 0.474$). Negative values indicate that, on average, the distribution of the left

Table 5: Design of KW and Conover statistical test results for inference latency comparison across the Operator(O) dimension, i.e., Identity(I), QAT, SPTQ, Pruned(P), Distilled(D), and DSTPQ within each of the Monolithic Deployment Tiers(T) for RQ1, RQ2, RQ3, and RQ4.

T \ O	I	QAT	SPTQ	P	D	DSPTQ
M	X	X	X	X	X	X
E						
C						

(a) Comparison across operators on Mobile(M) Tier

T \ O	I	QAT	SPTQ	P	D	DSPTQ
M						
E	X	X	X	X	X	X
C						

(b) Comparison across operators on Edge(E) Tier

T \ O	I	QAT	SPTQ	P	D	DSPTQ
M						
E						
C	X	X	X	X	X	X

(c) Comparison across operators on Cloud(C) Tier

member of the pair had lower values. The results provide insights into the comparative latency of each deployment strategy, especially concerning median values.

3.6.1 Tier Dimension

In Table 4, we conduct a KW test ($\alpha = 0.05$) to compare the inference latency of individual operators (Identity, Pruned, SPTQ, QAT, Distilled) across the three monolithic tiers (Mobile, Edge, Cloud) with the MEIP strategy. Similarly, we compare the inference latency of the hybrid operator (DSPTQ) across the MEC tiers with the MESP strategy. If significant differences are observed (KW Test: p-value < 0.05), we proceed with the Conover post-hoc test. In cases where there are notable differences (Conover test: adjusted p-value < 0.05) in pairwise comparisons, we use Cliff's delta effect size to gauge the inference latency ranking of strategies, considering the direction and magnitude of their differences in the relevant RQs.

3.6.2 Operator Dimension

For assessing the potential statistically significant differences among the Identity, QAT, SPTQ, Distilled, and DSPTQ operators within individual monolithic tiers, a Kruskal-Wallis (KW) test was conducted, as outlined in Table 5. In cases where a significant difference was detected (KW Test: p-value < 0.05), subsequent analysis employed the post-hoc Conover test. For significant pairwise comparisons (Conover test: adjusted p-value < 0.05), Cliff's delta effect size again was utilized to gauge the magnitude and direction of differences in inference latency ranks across relevant Research Questions (RQs).

For accuracy comparisons among operators, we utilize the Wilcoxon Signed Rank Test [24]. This test assesses the existence of a significant difference in accuracy between each pair of operators of interest such as Identity vs QAT, Identity vs SPTQ, QAT vs SPTQ, Pruning vs Identity, Pruning vs SPTQ, Pruning vs QAT, Distilled vs SPTQ, Distilled vs QAT, Distilled vs Pruned, Distilled vs Identity, DSPTQ vs SPTQ, DSPTQ vs QAT, DSPTQ vs Pruned, and DSPTQ vs Identity. The analysis focuses on paired groups, comparing accuracy measurements under different operators for the same subject models (ResNet, ResNext, Bert, Roberta) and environments (Mobile, Edge, Cloud). Each group comprises 18 samples of accuracy measurements, combining six accuracy metric values ([ResNet, ResNext] x [Top 1%, Top 5%] + [Bert, Roberta] x [F1 Score%]) across three environments. In other words, within a specific operator's group, we concatenate accuracy metric(s) – all percentage values – for all four subject models, facilitating the comparison of corresponding accuracy metrics through paired statistical tests.

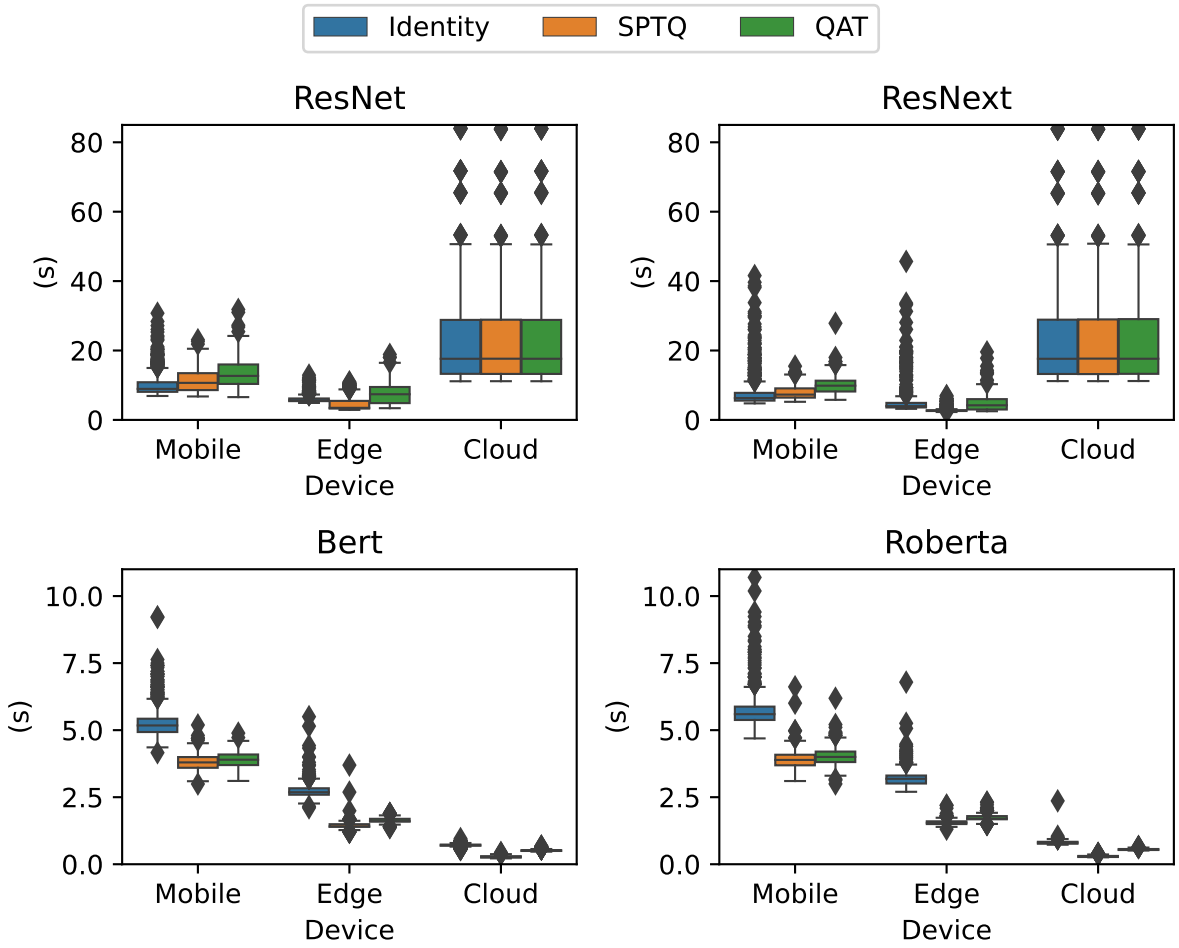

Fig. 4: Box plots of the measures collected for Inference Latency from Mobile, Edge, and Cloud tiers for Identity, SPTQ, and QAT versions of the subject models

To mitigate the risk of incorrect findings, we employ Bonferroni Correction [45] on the p-values in each Wilcoxon test, with an adjusted significance level of 0.01 considered as statistically significant. This threshold of 0.01 is determined by dividing the conventional significance level ($\alpha = 0.05$) by the number of multiple comparisons (5, as each operator is compared at most 5 times). Following this adjustment, if a noteworthy difference emerges between the two operators, we employ Cliff's Delta effect size [15] to gauge the extent and direction of their difference in the respective Research Questions (RQs).

After rounding off the decimal digits (up to 4 places) in the accuracy metric values, we observed that for each subject model, each of the 6 operators including hybrids (i.e., Identity, SPTQ, QAT, Pruned, Distilled, Distilled SPTQ) exhibits almost identical accuracy performance, as expected, between mobile and edge tiers, as shown in Table 9. The main reason seems to be the identical hardware (CPU processor) and software (packages) configuration of mobile and edge-simulated docker containers.

4 Results

4.1 What is the impact of the QAT-based white box operator on latency and accuracy? (RQ1)

The White-box QAT operator always has one of the longer median latencies in comparison to the black-box SPTQ operator, except for cloud image models.

In Mobile and Edge, the QAT models show 1.02x to 1.35x and 1.10x to 2.12x higher median inference latency, respectively than the SPTQ models, as shown in Figure 4 along with small or large effect sizes

(Table 6, Table 7). The SPTQ process is performed by the ONNX framework, while the generation of the QAT model is performed by the PyTorch framework, after which the generated QAT models are exported to the ONNX format for inference. The exportation process from PyTorch to ONNX for QAT operations may introduce additional steps, conversions, or variations that might be computationally expensive leading to slower latency during inference than the SPTQ models. In particular, the Fake Quantization Operations of QAT models compatible with Pytorch format are not supported in ONNX format, which might be the reason for QAT's slower latency. Moreover, in Edge, the SPTQ versions of image and textual subject models show 1.48x to 1.62x and 1.90x to 2.06x lower median inference latency than the identity version, along with large effect sizes (Table 7).

In contrast, the QAT versions of image and textual subject models show 1.06x to 1.31x higher (negligible to small effect size) and 1.67x to 1.87x lower (large effect sizes) median inference latency, respectively than the identity versions in the edge. For image subject models, the SPTQ versions can perform better than the identity versions in at least a high-resource environment (i.e., edge). However, the QAT image models perform worse in both high/low resource environments than the identity image models possibly due to the QAT model exportation factor as explained earlier.

In the cloud, there is no statistically significant inference latency difference between the Identity, SPTQ, and QAT versions for image subject models (Table 8). The main reason is the major impact of higher image data size and lower cloud bandwidth on the overall inference latency. However, for textual subject models, the identity versions show 1.38x to 1.47x and 2.55x to 2.78x higher median inference latency than the SPTQ and QAT versions, respectively along with large effect sizes (Table 8). The textual subject models have lower input data size requirements, due to which the impact on the overall inference latency is quite low. In other words, the significant difference observed between Quantized (QAT/SPTQ) and Identity textual models is due to the computational latency differences. The QAT/SPTQ textual models have lower model sizes and lower CPU/Memory requirements, which led them to perform more robustly than the identity textual models. Among the SPTQ and QAT textual models in the cloud, the SPTQ models show 1.83x to 1.88x lower median inference latency than the QAT models along with large effect sizes (Table 8). The QAT textual models are slower than the SPTQ textual models in the cloud, possibly due to the computational latency differences caused by the QAT model exportation process as explained earlier.

The QAT and SPTQ models in comparison to identity models show a small accuracy drop of 0.49% to 1.53% and 0.09% to 1.58%, respectively. Between the QAT and SPTQ operators themselves, there is no statistically significant difference in accuracy.

As shown in Table 9, the QAT versions wrt. Identity versions demonstrate an accuracy drop of 0.49% to 1.53% across all subject models, except Roberta, for which the QAT versions show an accuracy gain of 0.19% to 0.25%. In contrast, the SPTQ versions wrt. Identity versions show an accuracy drop of 0.09% to 1.58% across all 4 subject models. Wilcoxon tests affirm that the QAT vs Identity and SPTQ vs Identity accuracy difference is statically significant with a p-value of 0.0001 and $7.6e^{-6}$ ($\alpha = 0.01$), but, at a small effect size. The QAT vs SPTQ accuracy comparison indicates a drop of 0.29% to 1.3% for the QAT models across all subject models, except Roberta, for which the QAT model shows an accuracy gain of 1.13% to 1.78%. The Wilcoxon test states no significant difference among the QAT and SPTQ versions across the 4 subject models. The QAT performance depends on the models' characteristics and the training parameters. We used the default hyper-parameter values reported on the INC repository for the QAT operator, as stated in the RQ1 Approach. Our choice of default hyper-parameter values is inspired by existing work (Table 1) which majorly uses it (15 out of 17) while studying only the QAT operator. Performing more exhaustive training might give a better performance of the QAT operator in comparison to the SPTQ operator.

As stated in previous studies (Table 1), the QAT and SPTQ operators in our study also show a small (not significant) accuracy drop in comparison to the original model. In terms of comparison between QAT and PTQ operators, a previous study [131] shows that QAT produces better accuracy benefits than PTQ, but it suffers from a long training process. In our study, the QAT was slightly under-performed compared to SPTQ in terms of accuracy. To effectively recover the accuracy, the retraining process of QAT might require several hundred epochs, which incurs huge computational and training time costs for MLOps engineers. In contrast, the SPTQ process is a lightweight pipeline and doesn't require re-training or labeled data like QAT and showed similar accuracy performance compared to QAT at low cost (in terms of computational resources, time, and effort) in our study.

Table 6: Cliff's Delta effect size for latency comparison between Identity (I), SPTQ (Q1), QAT(Q2), Pruned (P), Distilled (D), and Distilled SPTQ (DQ1) versions of the subject models in the Mobile tier for RQ1, RQ2, RQ3, and RQ4

ResNext \ ResNet	I	Q1	Q2	P	D	DQ1
I	-	S	L		-L	-L
Q1	M	-	S	-S	-L	-L
Q2	L	-L	-	-L	-L	-L
P	N	M	L	-	-L	-L
D	L	L	L	L	-	N
DQ1	L	L	L	L	-M	-

Roberta \ Bert	I	Q1	Q2	P	D	DQ1
I	-	-L	-L		-L	-L
Q1	L	-	S	L	-L	-L
Q2	L	-S	-	L	-L	-L
P		-L	-L	-	-L	-L
D	L	L	L	L	-	-L
DQ1	L	L	L	L	L	-

[1] In these, and later, tables, a Positive sign for the i^{th} cell shows that the latency of column[i]>row[i], while a Negative sign for the i^{th} cell shows that the latency of column[i]<row[i].
[2] In these, and later, tables, the L, M, S, and N symbols mean Large, Medium, Small, and Negligible effect size, respectively.
[3] In these, and later, tables, an empty cell means that the cliff's delta effect size was not considered because the pairwise comparison was not statistically significant.

Table 7: Cliff's Delta effect size for latency comparison between Identity (I), SPTQ (Q1), QAT(Q2), Pruned (P), Distilled (D), and Distilled SPTQ (DQ1) versions of the subject models in the Edge tier for RQ1, RQ2, RQ3, and RQ4

ResNext \ ResNet	I	Q1	Q2	P	D	DQ1
I	-	-L	S	-S	-L	-L
Q1	L	-	L	L	-L	-L
Q2	N	-L	-	-S	-L	-L
P	S	-L		-	-L	-L
D	L	L	L	L	-	-L
DQ1	L	L	L	L	S	-

Roberta \ Bert	I	Q1	Q2	P	D	DQ1
I	-	-L	-L		-L	-L
Q1	L	-	L	L	-L	-L
Q2	L	-L	-	L	-L	-L
P	S	-L	-L	-	-L	-L
D	L	L	L	L	-	-L
DQ1	L	L	L	L	L	-

Summary of Research Question 1

For textual subject models, the SPTQ operator shows a speedup over the other 2 operators (Identity, QAT) in the Mobile (1.21x), Edge (1.55x), and Cloud (2.26x). For image subject models, the Identity and SPTQ operators show speedups in mobile (1.33x) and edge (1.70x), respectively over the other 2 operators, while in Cloud, no significant difference is observed. Regarding accuracy, the QAT and SPTQ operators show a small drop (<1.6%) relative to the Identity operator without significant differences when compared with each other.

Table 8: Cliff's Delta effect size for latency comparison between Identity (I), SPTQ (Q1), QAT(Q2), Pruned (P), Distilled (D), and Distilled SPTQ (DQ1) versions of the subject models in the Cloud tier for RQ1, RQ2, RQ3, and RQ4

ResNext \ ResNet	I	Q1	Q2	P	D	DQ1
I	-					
Q1		-				
Q2			-			
P						
D					-	
DQ1						-

Roberta \ Bert	I	Q1	Q2	P	D	DQ1
I	-	-L	-L	N	-L	-L
Q1	L	-	L	L	S	-L
Q2	L	-L	-	L	-L	-L
P	S	-L	-L	-	-L	-L
D	L	L	L	L	-	-L
DQ1	L	L	L	L	L	-

Table 9: Accuracy Performance of Identity, QAT, SPTQ, Pruned, Distilled, and Distilled SPTQ versions of subject models within Mobile, Edge, and Cloud tiers.

Subject Models	Operator	Model Size	Top-1%			Top-5%			F1 Score%		
			Mobile	Edge	Cloud	Mobile	Edge	Cloud	Mobile	Edge	Cloud
ResNet	Identity	484 MB	82.52	82.52	82.516	96.008	96.008	96.01	-	-	-
ResNet	SPTQ	123 MB	82.148	82.148	82.164	95.792	95.792	95.814	-	-	-
ResNet	QAT	123 MB	81.386	81.386	81.506	95.488	95.488	95.52	-	-	-
ResNet	Pruned	484 MB	81.35	81.35	81.35	95.63	95.63	95.634	-	-	-
ResNet	Distilled	263 MB	81.664	81.664	81.658	95.654	95.656	95.656	-	-	-
ResNet	Distilled SPTQ	67 MB	81.184	81.184	81.2	95.508	95.508	95.538	-	-	-
ResNext	Identity	319 MB	83.244	83.244	83.246	96.456	96.456	96.458	-	-	-
ResNext	SPTQ	81 MB	83.084	83.084	83.14	96.402	96.402	96.386	-	-	-
ResNext	QAT	81 MB	81.922	81.922	81.838	95.878	95.878	95.744	-	-	-
ResNext	Pruned	319 MB	80.978	80.978	80.978	95.678	95.678	95.676	-	-	-
ResNext	Distilled	96 MB	80.786	80.786	80.782	95.24	95.24	95.24	-	-	-
ResNext	Distilled SPTQ	25 MB	80.466	80.466	80.46	95.044	95.044	95.138	-	-	-
Bert	Identity	418 MB	-	-	-	-	-	-	90.42	90.42	90.42
Bert	SPTQ	107 MB	-	-	-	-	-	-	89.631	89.631	89.51
Bert	QAT	107 MB	-	-	-	-	-	-	88.889	88.889	88.889
Bert	Pruned	418 MB	-	-	-	-	-	-	88.621	88.621	88.621
Bert	Distilled	110 MB	-	-	-	-	-	-	88.285	88.285	88.285
Bert	Distilled SPTQ	29 MB	-	-	-	-	-	-	88.165	88.165	87.905
Roberta	Identity	476 MB	-	-	-	-	-	-	91.379	91.379	91.379
Roberta	SPTQ	122 MB	-	-	-	-	-	-	90.508	90.508	89.796
Roberta	QAT	122 MB	-	-	-	-	-	-	91.638	91.638	91.579
Roberta	Pruned	476 MB	-	-	-	-	-	-	88.962	88.962	88.962
Roberta	Distilled	107 MB	-	-	-	-	-	-	88.889	88.889	88.889
Roberta	Distilled SPTQ	28 MB	-	-	-	-	-	-	88.07	88.07	88.455

4.2 What is the impact of the Pruning-based white box operator on latency and accuracy? (RQ2)

The Pruned models show no practically significant latency improvements compared to Identity models in the MEC tiers. For the image subject models, the Pruned versions in MEC tiers show 1.55x/1.22x lower, 1.22x lower/1.49x higher, and equivalent average median inference latency than the QAT/SPTQ version, respectively. For the textual subject models, the Pruned versions show 1.36x/1.39x, 1.74x/1.95x, and 1.41x/2.63x higher average median inference latency than the QAT/SPTQ versions in the same tiers.

The inference latency of the pruned versions of the subject models, when compared with the identity version, shows either no significant difference or a significant difference but with negligible to small effect sizes in the monolithic tiers (i.e., mobile, edge, cloud) as shown in Table 6, Table 7, and Table 8. Further-

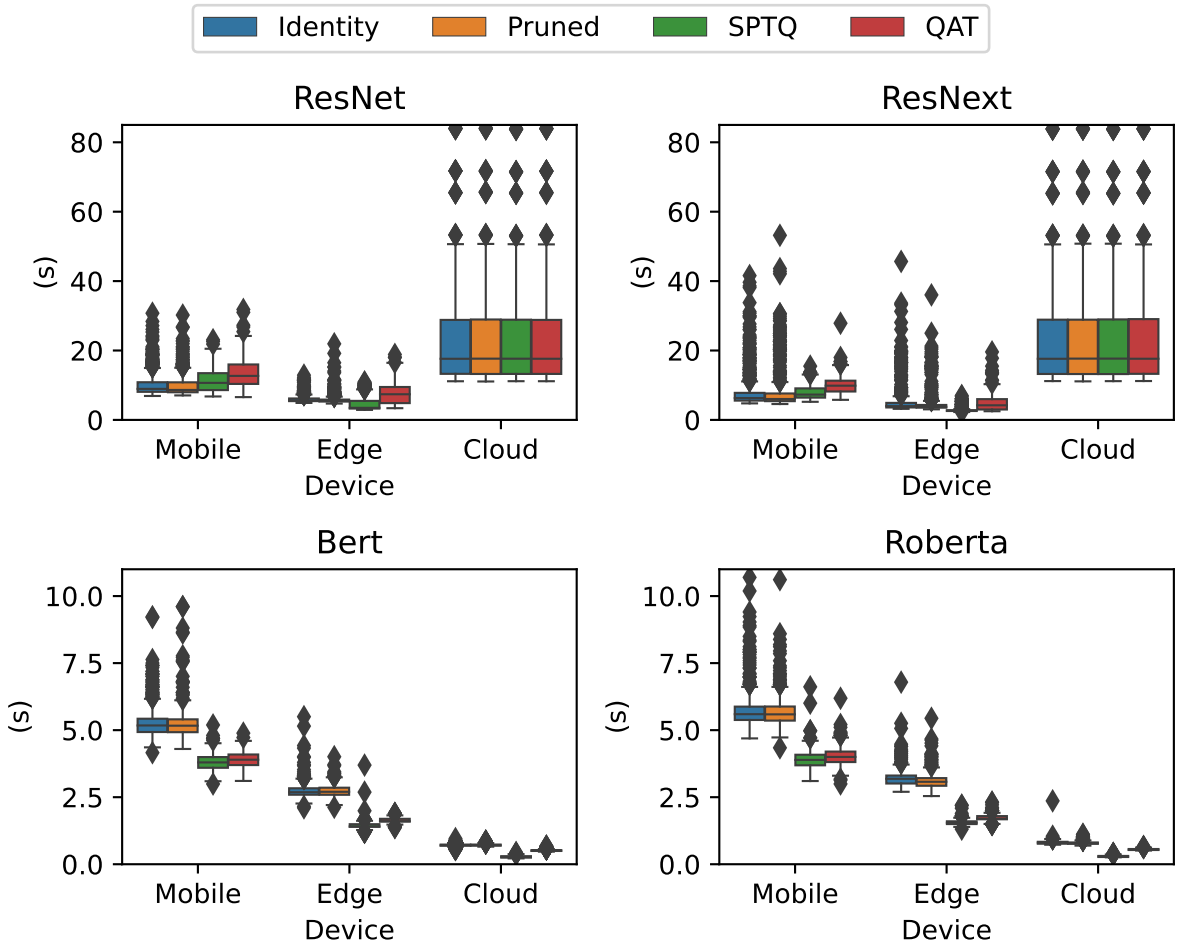

Fig. 5: Box plots of the measures collected for Inference Latency of Identity, Pruned, SPTQ, and QAT models in monolithic deployment tiers

more, the median inference latency differences between Identity and pruned models in the monolithic tiers are quite low (Figure 5). The pruned models show no reduction in model size compared to identity models as shown in Table 9, due to which the latency difference is practically insignificant.

In Mobile, for image subject models, the Pruned versions show 1.46x to 1.63x and 1.21x to 1.23x lower median inference latency than the QAT and SPTQ versions, respectively as shown in Figure 4, along with small to large effect sizes (Table 6). In contrast, for textual subject models, the Pruned versions show 1.32x to 1.39x and 1.36x to 1.43x higher median inference latency than the QAT and SPTQ versions, respectively along with large effect sizes.

In Edge, the Pruned versions for image and textual subject models show 1.41x to 1.58x and 1.68x to 1.80x higher median inference latency than the SPTQ versions along with large effect sizes (Table 7). For image and textual subject models, the Pruned versions show 1.11x to 1.33x lower (no significant difference or significant difference with small effect size) and 1.68x to 1.80x higher (large effect sizes) median inference latency, respectively than the QAT version.

In the Cloud, no statistically significant inference latency difference exists between the Pruned and QAT/SPTQ versions of image subject models (Table 8). However, for the textual subject models, the Pruned versions show 1.39x to 1.43x and 2.55x to 2.70x higher median inference latency than the QAT and SPTQ versions, respectively along with large effect sizes (Table 8).

The reasoning for latency differences between Pruned and SPTQ/QAT models in monolithic tiers is similar to Identity vs QAT/SPTQ latency comparison in monolithic tiers as explained in RQ1 findings (Section 4.2).

The Pruned models cost a medium accuracy drop in comparison to Identity models. Regarding the Pruned model's performance against QAT and SPTQ models, a small drop and a medium drop are shown, respectively.

The pruned models show an accuracy drop of 0.376% to 2.417% (Wilcoxon Test: p-value = $7.6e^{-6}$, α = 0.01) in comparison to identity models as presented in Table 9 along with medium effect size. Moreover, the Pruned models demonstrate an accuracy drop of 0.03% to 2.67% (Wilcoxon Test: p-value = 0.001, α = 0.01) at a small effect size and an accuracy drop of 0.16% to 2.16% (Wilcoxon Test: p-value = $7.6e^{-6}$, α = 0.01) at medium effect size when compared with QAT and SPTQ models, respectively as shown in Table 9. This finding suggests that pruned models are ineffective in improving performance relative to Identity, SPTQ, and QAT models.

In previous pruning studies (Table 1), the physical pruning method reduces the model size and parameters by removing the pruned weights without any significant effect on the accuracy performance compared to the original model, which results in faster latency performance during deployment. The choice of frameworks considered for physical pruning in previous studies is either PyTorch or TensorFlow. Our reason to instead consider logical pruning using the INC tool is briefly discussed in the RQ2 Approach Section 3.5.2. The accuracy of the pruned models shows a significant (medium) loss, possibly due to high sparsity% during training.

In a recent study [48], comparing compression techniques, Quantization generally outperforms Pruning in most cases. Only in some scenarios with a very high compression ratio, pruning was found to be beneficial from an accuracy standpoint. In another study [59], the choice of compression technique is strongly model-dependent. In our study, the pruned versions show small to medium accuracy loss in comparison to Quantized versions (SPTQ, QAT) across the four subject models (i.e., choice of compression technique is not model-dependent).

Summary of Research Question 2

The Pruned operator shows practically insignificant latency differences in the monolithic tiers, at a medium accuracy drop (up to ≈2.5%) relative to the Identity operator.
For textual subject models, the Pruned operator slows down w.r.t the QAT/SPTQ operator in Mobile (1.36x/1.39x), Edge (1.74x/1.95x), and Cloud (1.41x/2.63x). In contrast, for image subject models, the Pruned operator speeds up in Mobile (1.55x/1.22x), and speeds up/slows down in Edge (1.22x/1.49x), while in cloud, no significant difference is observed. The Pruned operator shows a small/medium accuracy drop (<2.7%) wrt QAT/SPTQ operators.

4.3 What is the performance impact of the Distillation-based white box operator on latency and accuracy? (RQ3)

Except for cloud image models, the distilled models in comparison to the Identity/QAT/SPTQ/Pruned models show significantly lower latency with large effect sizes.

As shown in Figure 6 7, the Distilled models in the mobile tier show 3.39x, 3.36x, 2.94x, and 3.34x lower average median inference latency than the Identity, QAT, SPTQ, and Pruned models, respectively along with large effect sizes (Table 6). Similarly, in the edge tier, the distilled models show 3.39x, 2.66x, 1.90x, and 3.31x lower average median inference latency than the Identity, QAT, SPTQ, and Pruned models, respectively along with large effect sizes (Table 7). In Figure 7, the speedup of Distilled models w.r.t. Identity, QAT, SPTQ, and Pruned models is calculated by comparing their median latency with each other. For example, the box plots in Figure 6 show that the Distilled versions w.r.t. Identity versions in the mobile tier have 1.76 to 4.73 times lower (speedup) median inference latency values across the four subject models. To present this quantitatively, we use the orange lines and red dots in the interval plot 7 to illustrate the speedup range (1.76x to 4.73x) and average (3.39x), respectively across the four subject models (as these values are greater than one). In contrast, for showing slow down, the interval plots show values smaller than one, as illustrated in other interval plots (e.g., Fig 9,10). The Distilled models are 1.84x to 4.44x smaller in size than the Identity/Pruned models as shown in Table 9, leading to faster and more efficient inference of Distilled models in restricted-constrained tiers (i.e., mobile and edge) in comparison to Identity/Pruned models. Even though the distilled model sizes of the subject models

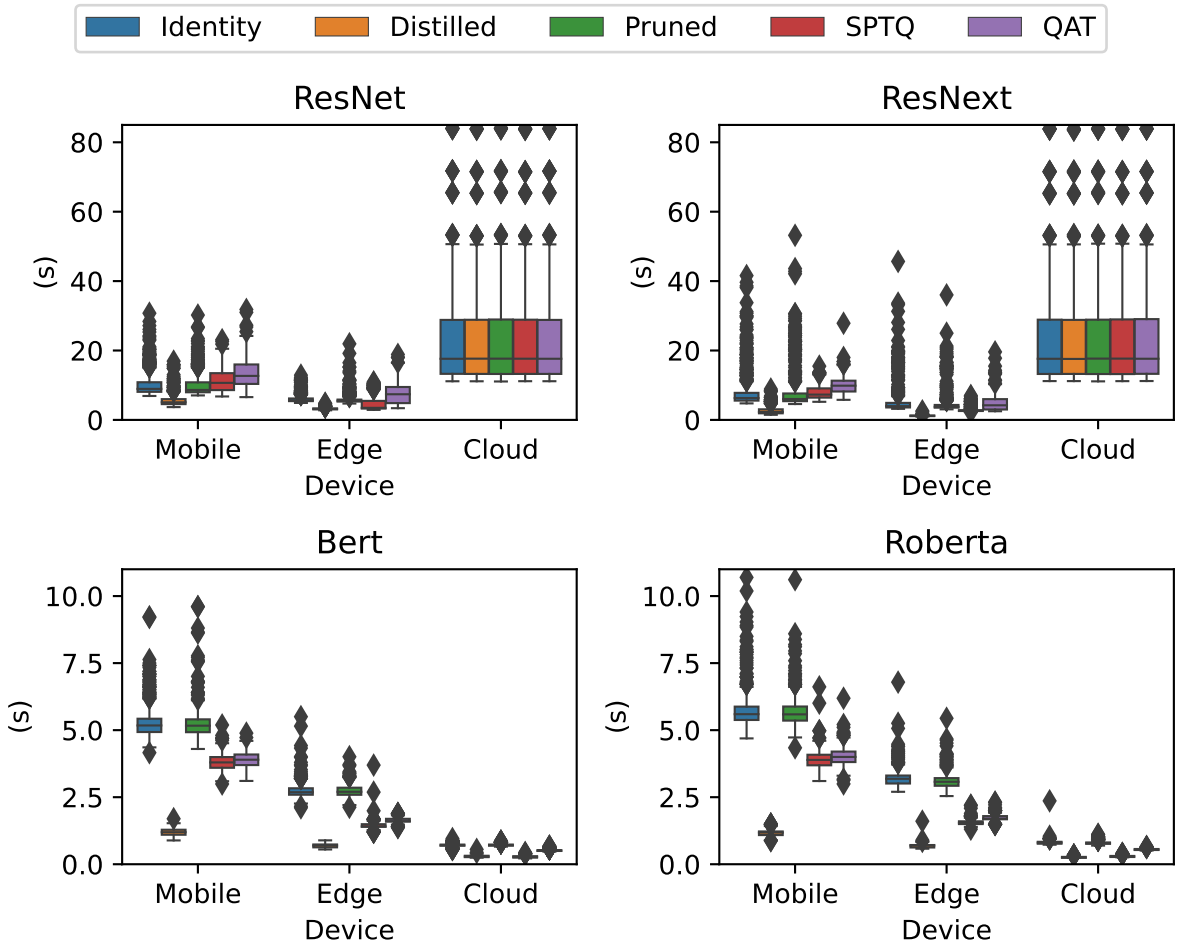

Fig. 6: Box plots of the measures collected for Inference Latency of Identity, Distilled, Pruned, SPTQ, and QAT models in monolithic deployment tiers

(except Roberta) are 1.02x to 2.1x higher than the QAT/SPTQ models, they still show better latency results than QAT/SPTQ models possibly due to architectural simplicity, fewer model parameters, and lower computational/memory requirements of distilled models.

According to the Conover test, the null hypothesis that there is no significant difference between the Distilled and Identity/SPTQ/QAT/Pruned versions in the Cloud cannot be rejected for image subject models, indicating that their comparison during Cloud deployment shows similar or equivalent inference latency. The main reason for this finding is the impact of network bandwidth and image data size on the overall inference latency during Cloud deployment. For the textual subject models, the Distilled versions show 2.84x, 1.98x, and 2.8x lower average median inference latency in comparison to Identity, QAT, and Pruned versions, respectively in the cloud as shown in Figure 8 (orange, blue, red, and brown box plots) along with large effect sizes (Table 8). Similarly, for Roberta, the Distilled versions in comparison to the SPTQ versions show 1.16x lower median inference latency in the Cloud along with a large effect size. For Bert, the Distilled versions show slightly higher (1.03x) median inference latency than its SPTQ version, but, the effect size remains small, meaning the difference is not practically significant. The simpler architecture, lower model parameters, lower computational/memory requirements, and/or smaller model size of distilled textual models in comparison to Identity/QAT/SPTQ/Pruned models speeds up the computation latency in the cloud, while the smaller size of input textual data does not impact the inference latency.

The Distilled models show small to medium accuracy drops when compared with the Identity, QAT, and SPTQ models (except Pruned models).

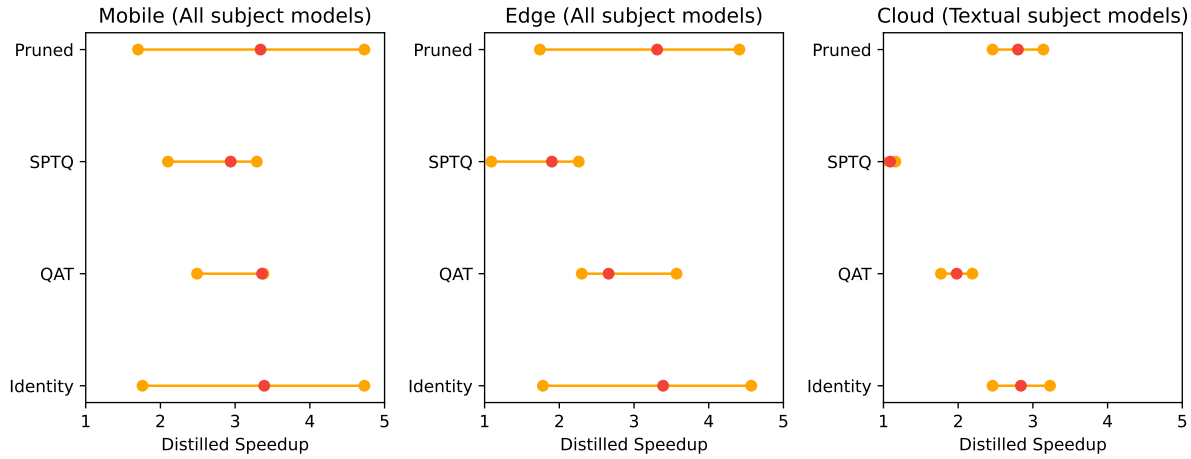

Fig. 7: Interval Plots presenting the median inference latency speedup in terms of average (red dot) and range (orange line) across the subject models for Distilled versions w.r.t. Pruned, SPTQ, QAT, and Identity versions in Monolithic Deployment tiers. For example, a dot on 3.0 indicates a 3-fold speedup of a distilled version compared to another model version.

The Distilled model's accuracy when compared with Identity, QAT, and SPTQ models shows drops of 0.35% to 2.49% (Wilcoxon Test: p-value = $7.6e^{-6}$, $\alpha = 0.01$) at a medium effect size, 0.5% to 2.74% (Wilcoxon Test: p-value = 0.003, $\alpha = 0.01$) at a small effect size, and 0.21% to 2.17% (Wilcoxon Test: p-value = $7.6e^{-6}$, $\alpha = 0.01$) at a medium effect size, respectively. Moreover, the distilled models compared to Pruned models show statistically insignificant differences as per the Wilcoxon Test, meaning their accuracy performance is similar.

In previous studies (Table 1) considering Knowledge Distillation, the model size is also reduced substantially, resulting in lower latency at a small accuracy loss. In contrast, in our study, the Knowledge Distillation shows faster latency, but at medium accuracy loss. The accuracy performance depends on the hyper-parameters used while training and might be improved by tuning these hyper-parameters. In a recent paper [82], QAT yields the best accuracy-compression trade-offs, followed by Knowledge Distillation and then Pruning. In our study, the Knowledge Distillation operator is a better alternative when faster latency is a concern in resource-constrained tiers at insignificant accuracy difference compared to Pruned models and small/medium accuracy loss compared to QAT/SPTQ models.

Summary of Research Question 3

The Distilled operator could be the preferred choice over the Identity, QAT, SPTQ, and Pruned operator when faster latency is a concern in the Mobile (3.39x/3.36x/2.94x/3.34x), Edge (3.39x/2.66x/1.90x/3.31x), and Cloud (2.84x/1.06x/1.98x/2.80x for textual subject models) tiers at medium(up to 2.49%), small(up to 2.74%), medium(up to 2.17%), and insignificant accuracy loss, respectively.

4.4 What is the impact of the hybrids of white-box and/or black-box operators on latency and accuracy? (RQ4)

4.4.1 Quantitative Analysis of hybrid Distilled SPTQ (DSPTQ) operator with singular Distilled, SPTQ, QAT, Pruned, and Identity operators in Monolithic Deployment tiers

Except for cloud and mobile image models, the DSPTQ models show significantly lower latency than the distilled models with small to large effect sizes.

As shown in Figure 8 9, in the mobile tier, for the image and textual subject models, the DSPTQ versions show 1.19x higher (negligible or medium effect sizes) and 1.39x lower (large effect sizes) average

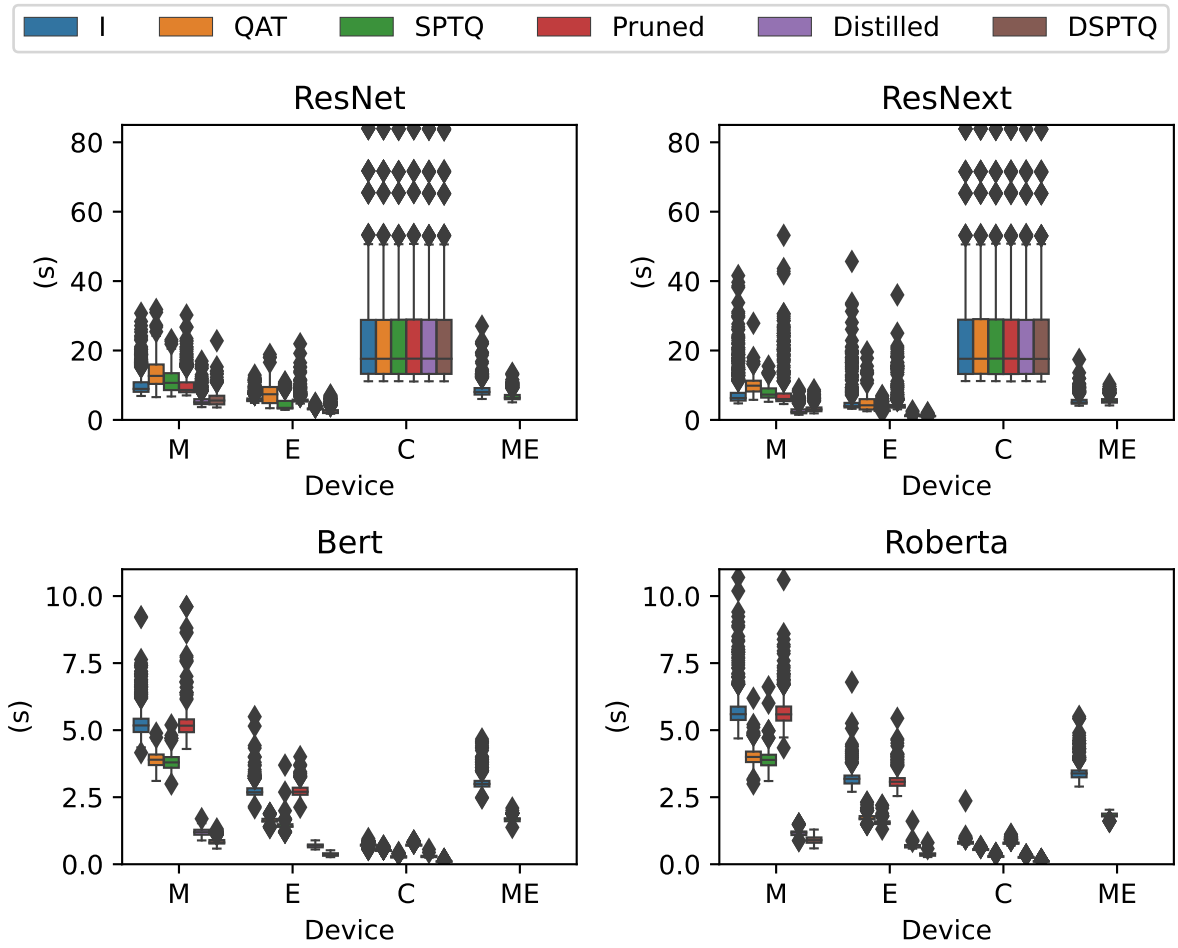

Fig. 8: Box plots of the Inference Latency measure for Identity(I), QAT, SPTQ, Pruned, Distilled and Distilled SPTQ (DSPTQ) in Monolithic Deployment tiers and Mobile-Edge (ME) Identity/SPTQ Partitioning strategy.

median inference latency, respectively, than the distilled versions (Table 6). However, in the edge tier, for both image and textual subject models, the DSPTQ versions exhibit 1.29x (small to large effect sizes) and 1.76x (large effect sizes) lower average median inference latency than the distilled versions (Table 7). The speedup of the DSPTQ operator in Figure 9 is calculated by comparing it with other operators in terms of median latency, as explained previously for Figure 7 (see first finding in Section4.3). Even though the DSTPQ image models have a 3.84x to 4x lower size than the distilled image models, still they show lower latency in the mobile tier, which indicates that their Quantization Operations are costly in lower Memory/CPU environments.

In contrast, the faster latency of DSPTQ textual models in both mobile and edge tiers indicates that their Quantization operations can be performed effectively in both lower and higher CPU/Memory environments possibly due to their lower resource utilization during inference. Lastly, in the cloud, the DSPTQ image models when compared with distilled image models show no statistically significant difference possibly due to the high influence of low cloud network bandwidth and the higher image sample sizes on inference latency. However, the DSPTQ textual models in the cloud show 2.36x to 2.90x lower (large effect sizes) average median inference latency than the Distilled textual models because of their lower influence on transmission latency due to lower textual data size and higher influence on computational latency due to lower model size, model parameters, and CPU/memory requirements.

Except for cloud image models, the DSPTQ models in comparison to the SPTQ, QAT, Pruned, and Identity models show significantly lower latency with large effect sizes.

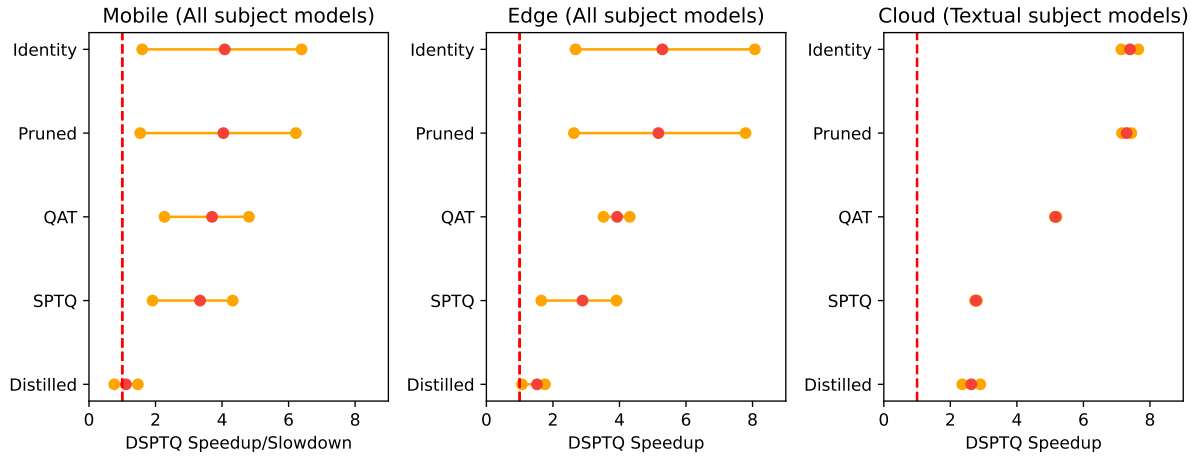

Fig. 9: Interval Plots presenting the median inference latency speedup in terms of average (red dot) and range (orange line) across the subject models for DSPTQ versions w.r.t. Identity, Pruned, QAT, SPTQ, and Distilled versions in Monolithic Deployment tiers. For example, a dot on 3.0 indicates a 3-fold speedup of a DSPTQ model version compared to another model version, while any dot on the left of the red line indicates a slowdown (improvement lower than 1.0). Note that for the Cloud tier, we only show the results for textual subject models, because they show significant differences in latency.

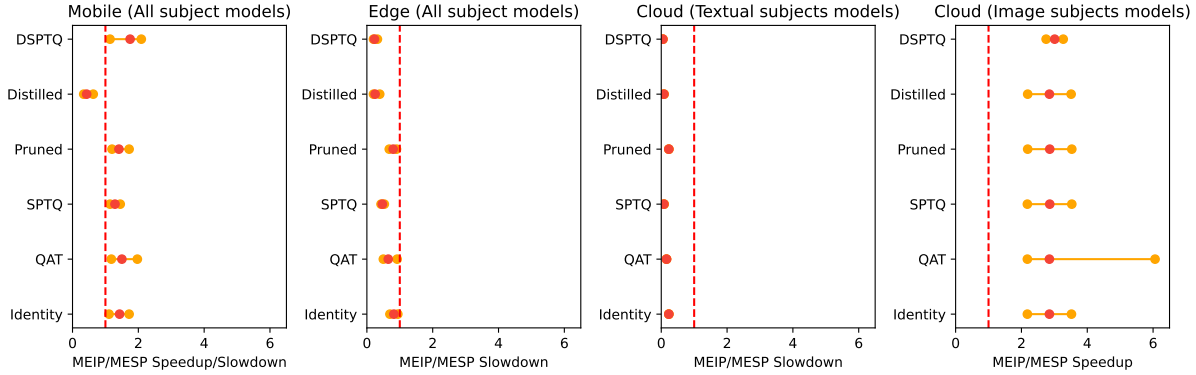

Fig. 10: Interval Plots presenting the median inference latency speedup/slowdown in terms of average (red dot) and range (orange line) across the subject models for MEIP/MESP strategies w.r.t. DSPTQ, Distilled, Pruned, SPTQ, QAT, and Identity Monolithic Deployment strategies. (For example, a dot on 3.0 indicates a 3-fold speedup of a MEIP/MESP model version compared to another model version, while any dot on the left of the red line indicates a slowdown (improvement lower than 1.0)

As shown in Figure 9, the DSPTQ models show 3.34x, 3.7x, 4.04x, and 4.08x lower average median inference latency in mobile; 2.89x, 3.93x, 5.17x, and 5.29x lower average median inference latency in edge, in comparison to SPTQ, QAT, Pruned, and Identity models, respectively. Similarly, in the cloud, for the textual subject models, the DSPTQ models show 2.77x, 5.16x, 7.30x, and 7.40x lower average median inference latency when compared with the same models. The DSPTQ models in comparison to SPTQ, QAT, Pruned, Identity models show significantly lower latency along with large effect sizes for all subject models in resource-constrained tiers (Table 6, 7) and for textual subject models in cloud tier (Table 8). However, for image subject models, the DSPTQ models in the cloud show no statistically significant differences relative to SPTQ, QAT, Pruned, and Identity models. This is due to the major influence of high image size and low cloud network bandwidth on the overall inference latency.

Regarding accuracy, the DSPTQ models show a small to medium accuracy drop relative to the Distilled, SPTQ, QAT, Pruned, and Identity models.

Based on the Wilcoxon Test (p-value = $7.6e^{-6}$, $\alpha = 0.01$), the DSTPQ model's accuracy performance when compared with Distilled, SPTQ, QAT, Pruned, and Identity models shows a significant difference with accuracy drops of 0.10% to 0.81%, 0.33% to 2.49%, 0.2% to 3.56%, 0.09% to 0.89%, and 0.47% to 3.30%, respectively. Moreover, the DSTPQ models show small (w.r.t. Distilled, QAT, Pruned) to medium (w.r.t. SPTQ, Identity) effect sizes.

In previous studies [56,106,54,9,82], the hybrid operator (Knowledge Distillation + Quantization) gives a significant accuracy performance boost over the Quantized operator while achieving model size reduction. In contrast, in our study, this hybrid operator shows small to medium accuracy loss compared to Quantized variants. This can be improved by hyper-parameter tuning during the training process of Distillation and Quantization.

4.4.2 Quantitative Analysis of MEIP strategy with Identity/QAT/SPTQ/Pruned/Distilled models and MESP strategy with DSPTQ models

Table 10: Cliff's Delta effect size for latency comparison between Mobile (M), Edge (E), Cloud (C) for Identity models (I_t, I_x, I_b, I_r denote identity versions of ResNet, ResNext, Bert, Roberta) and the MEIP strategy for RQ4 and Discussion Section

I_x \ I_t	M	E	C	MEIP
M	-	-L	L	-M
E	L	-	L	L
C	-L	-L	-	-L
MEIP	L	-L	L	-

I_r \ I_b	M	E	C	MEIP
M	-	-L	-L	-L
E	L	-	-L	L
C	L	L	-	L
MEIP	L	-L	-L	-

Table 11: Cliff's Delta effect size for latency comparison between Mobile (M), Edge (E), Cloud (C) Deployment for SPTQ models ($SPTQ_t$, $SPTQ_x$, $SPTQ_b$, $SPTQ_r$ denote SPTQ versions of ResNet, ResNext, Bert, Roberta) and the MEIP strategy for RQ4 and Discussion Section.

$SPTQ_x$ \ $SPTQ_t$	M	E	C	MEIP
M	-	-L	L	-L
E	L	-	L	L
C	-L	-L	-	-L
MEIP	L	-L	L	-

$SPTQ_r$ \ $SPTQ_b$	M	E	C	MEIP
M	-	-L	-L	-L
E	L	-	-L	L
C	L	L	-	L
MEIP	L	-L	-L	-

Table 12: Cliff's Delta effect size for latency comparison between Mobile (M), Edge (E), and Cloud (C) Deployment for QAT models (QAT_t, QAT_x, QAT_b, QAT_r denote QAT versions of ResNet, ResNext, Bert, Roberta) and the MEIP strategy for RQ4 and Discussion Section.

QAT_x \ QAT_t	M	E	C	MEIP
M	-	-L	L	-L
E	L	-	L	S
C	-L	-L	-	-L
MEIP	L	-S	L	-

QAT_r \ QAT_b	M	E	C	MEIP
M	-	-L	-L	-L
E	L	-	-L	L
C	L	L	-	L
MEIP	L	-L	-L	-

The Identity/QAT/SPTQ/Pruned models w.r.t MEIP strategy show significantly higher (in mobile) and lower (in edge) latency with small to large effect sizes. The same models in the cloud show significantly higher and lower latency for image and textual tasks, respectively than the same strategy with large effect sizes.

Table 13: Cliff's Delta effect size for latency comparison between Mobile (M), Edge (E), and Cloud (C) Deployment for Pruned models (P_{t}, P_{x}, P_{b}, P_{r} denote pruned versions of ResNet, ResNext, Bert, Roberta) and the MEIP strategy for RQ4 and Discussion Section.

P_{x} \ P_{t}	M	E	C	MEIP
M	-	-L	L	-S
E	L	-	L	L
C	-L	-L	-	-L
MEIP	L	-L	L	-

P_{r} \ P_{b}	M	E	C	MEIP
M	-	-L	-L	-L
E	L	-	-L	L
C	L	L	-	L
MEIP	L	-L	-L	-

Table 14: Cliff's Delta effect size for latency comparison between Mobile (M), Edge (E), and Cloud (C) Deployment for Distilled models (D_{t}, D_{x}, D_{b}, D_{r} denote distilled versions of ResNet, ResNext, Bert, Roberta) and the MEIP strategy for RQ4 and Discussion Section.

D_{x} \ D_{t}	M	E	C	MEIP
M	-	-L	L	L
E	L	-	L	L
C	-L	-L	-	-L
MEIP	-L	-L	L	-

D_{r} \ D_{b}	M	E	C	MEIP
M	-	-L	-L	L
E	L	-	-L	L
C	L	L	-	L
MEIP	-L	-L	-L	-

Table 15: Cliff's Delta effect size for latency comparison between Mobile (M), Edge (E), and Cloud (C) Deployment of Distilled SPTQ models ($DSPTQ_{\text{t}}$, $DSPTQ_{\text{x}}$, $DSPTQ_{\text{b}}$, $DSPTQ_{\text{r}}$ denotes Distilled SPTQ versions of ResNet, ResNext, Bert, Roberta) and Mobile-Edge SPTQ Partitioning (MESP) strategy for RQ4 and Discussion Section.

$DSPTQ_{\text{x}}$ \ $DSPTQ_{\text{t}}$	M	E	C	MESP
M	-	-L	L	M
E	L	-	L	L
C	-L	-L	-	-L
MESP	-L	-L	L	-

$DSPTQ_{\text{r}}$ \ $DSPTQ_{\text{b}}$	M	E	C	MESP
M	-	-L	-L	L
E	L	-	-L	L
C	L	L	-	L
MESP	-L	-L	-L	-

The Identity, QAT, SPTQ, and Pruned models in mobile exhibit 1.43x, 1.50x, 1.29x, and 1.41x higher (medium to large effect sizes) and in edge exhibit 1.21x, 1.53x, 2.12x, and 1.24x lower (small or large effect sizes) average median inference latency, respectively than the MEIP strategy, as shown in Figure 8, 10 and Table 10, 11, 12, 13. For textual subject models, the same models when deployed in the Cloud also show 4.23x, 6.06x, 11.30x, and 4.29x lower average median inference latency relative to the MEIP strategy, along with large effect sizes. The speedup/slowdown of the MEIP/MESP strategies in Figure 10 is calculated by comparing the median latency with other operators, as explained earlier (see first finding in Section4.3) for Figure 7.

On the one hand, the deployment of the partition operator across resource-constrained tiers (i.e., Mobile and Edge) is more effective than deploying the entire model (Identity, QAT, SPTQ, Pruned) solely on the resource-constrained Mobile tier, due to the distribution of CPU/Memory load during inference. On the other hand, a partition operator may not be necessary for scenarios where a monolithic deployment tier (i.e., edge, cloud) is sufficiently capable of handling the computational load of the entire model, given that the impact of input data size and network bandwidth on the inference latency is low.

Conversely, for image subject models, the Cloud Identity, QAT, SPTQ, and Pruned models show 2.85x, 2.85x, 2.86x, and 2.86 higher average median inference latency than the MEIP strategy, along

with large effect sizes. This is due to the major impact of higher image data size and lower cloud network bandwidth on the overall inference latency.

Except for cloud image models, the Distilled and DSPTQ models show significantly lower latency than the MEIP and MESP strategies, respectively along with medium to large effect sizes.

As shown in Figure 8, 10, the Distilled/DSPTQ (image and textual-based) models during both Mobile and Edge deployment show 2.28x/1.75x and 3.98x/4.19x lower average median inference latency than the MEIP/MESP strategy along with medium to large effect sizes (Table 14, 15. Similarly, during Cloud deployment, the Distilled/DSPTQ textual models show 12.05x/17.18x lower average median inference latency than the MEIP/MESP strategy, along with large effect sizes. This suggests that the deployment of Distilled and DSPTQ operators across all subject models in resource-constrained tiers (mobile and edge) and the cloud tier for textual subject models can be an optimized choice when faster inference is a concern for MEIP and MESP strategies, respectively possible due their simpler architecture, lower model size/parameters and lower CPU/Memory requirements.

Conversely, for image subject models, the Cloud Distilled/DSTPQ models show 2.85x/3.01x higher median inference latency than the MEIP/MESP strategy along with large effect sizes possibly due to the impact of lower network bandwidth and higher image data size on the overall inference latency.

Summary of Research Question 4

The DSPTQ hybrid operator could be the preferred choice over the non-hybrid operators (i.e., Distilled/SPTQ/QAT/Pruned/Identity) in the Edge tier across all subject models when lower latency (1.52x/2.89x/3.93x/5.17x/5.29x) is a concern, at a small to medium accuracy loss.

5 Discussion

Across the three monolithic tiers, the operators (Identity,QAT, SPTQ, Pruned, Distilled, DSTPQ) for textual subject models in the cloud and image subject models in the edge show 3.54x to 9.43x and 2.65x to 7.44x lower latency, respectively compared to the remaining two tiers.

For textual models, as shown in Figure 6, the Identity, QAT, SPTQ, Pruned, Distilled and DSPTQ models in the cloud show 3.82x to 7.36x, 3.12x to 7.71x, 5.11x to 13.78x, 3.83x to 7.33x, 2.44x to 4.74x, and 3.75x to 8.55x lower median inference latency compared to their inference in the resource-constrained tiers (i.e., mobile and edge), respectively, along with large effect sizes (Table 10,11,12,13,14,15). This is because the cloud tiers provide faster computational latency due to higher Memory/CPU availability than resource-constrained tiers (i.e., mobile and edge) and faster transmission latency across the edge-cloud network for textual models having low data size requirements.

For image models, the Identity, QAT, SPTQ, Pruned, Distilled, and DSPTQ models in edge exhibit 1.58x to 4.43x, 3.12x to 7.71x, 2.73x to 6.61x, 1.56x to 4.67x, 1.60x to 14.92x, and 2.66x to 16x lower median inference latency compared to their inference in the remaining 2 tiers (mobile, cloud) as shown in Figure 8 along with large effect sizes (Table 10,11,12,13,14,15). This is because the edge tier has higher Memory/CPU availability than mobile and faster data transmission capabilities than the cloud for large-sized image samples due to its closer proximity to mobile.

In general, this suggests that the edge and cloud tiers could be the preferred choice for image and textual models, respectively, in deployment scenarios where computational limitations, bandwidth limitations, and input data size influence the overall inference latency.

The white-box operators require automated pipelines, whereas, for black-box Partioning-based operators, manual analysis is performed.

In terms of effort, using an automated tool like Intel Neural Compressor for applying white-box operators like QAT, Pruning, and Distillation suggests a streamlined and automated process. This implies that, right now, these operators can be performed without manual effort and intervention, as the tool automates the necessary modifications to achieve these while training the model. On the other hand, applying the Partitioning on Identity/SPTQ models currently requires manual analysis of the ONNX

computational graphs using the Netron Visualizer tool [18] and manual modifications of the neural network using ONNX Python APIs. The feasibility and the challenges of automating the black-box operators involving partitioning might vary for models with different ONNX computational graph architectures and complexities. The manual feasibility analysis of partitioning-based operators for ONNX models across different domains (i.e., CV, NLP) will help the MLOps Engineers check if it is worth investing time/resources for automating this in the future.

The white-box operators require longer training time, whereas, for black-box operators like SPTQ, the process is less costly in terms of time complexity.

The pruning and distillation of image subject models was conducted with 8 distributed GPUs to speed up the training time which took around 1 to 2 days because of higher training data size, higher training iterations, and higher computational/memory cost of image model training. For pruning/distillation of textual subject models, the training time was quite faster (4 to 7 minutes) even with single GPU/CPU support possibly due to factors like lower training data size, lower training iterations, and lower computational/memory cost of textual model training. For textual subject models, the SPTQ operator took 1-2 minutes and the QAT operator took around 30 minutes. Similarly, for image subject models, the QAT operator took 4.4 to 7.1 hours and the SPTQ operator took 1.3 to 1.6 hours. We can observe that the QAT operator is more costly in terms of time complexity than the SPTQ operator. This is because the QAT involves simulating the effects of quantization during the training process, which requires additional computations in both forward and backward passes leading to longer training time. In contrast, SPTQ just involves quantizing the pre-trained model without a training process. For QAT/ SPTQ operators, the quantization process was performed with CPU as it is not supported in GPU.

Previous studies consider hybrids of Pruning and Quantization with each other or in combination with Knowledge Distillation for preserving accuracy performance. In contrast, in our study, the combinations with (logical) Pruning were not considered due to its costly performance in terms of both accuracy and latency.

The Hybrid of the three white box operators proposed in [55,57] was more effective in accuracy performance than the QAT operator. In [82], when Quantization Aware Training and Pruning are used together, they amplify each other's accuracy losses. However, combining all three operators (i.e., also using Knowledge Distillation) preserves accuracy. In [41], quantization-aware pruning results in more computationally efficient models than either pruning or quantization alone. In [39,97,38,113,123,46], the combination of Quantization and Pruning boosts the model compression rate by a large margin without incurring accuracy loss. In our study, the INC framework does logical pruning, which in terms of size is less efficient than physical pruning, i.e., the weights occupy the same memory space whether their values are zero or not. Logical pruning is faster to implement as it does not require additional packages for removing the zero weights and is more widely used across a wide range of subject models in the INC tool. Therefore, in our study, the combination of Pruning and Quantization was not considered, as the pruning operator was not giving accuracy or latency benefits.

6 Threats to Validity

Below, we discuss threats to the study validity and the strategies we applied to mitigate these threats, based on literature guidelines [119].

Construct Validity: One possible threat is the mono-operation bias caused by having only one factor of network bandwidth, computational configuration (RAM/CPU), hyper-parameters, and Partitioning point. Mobile-edge network bandwidth was set to 200 Mbps, and edge-cloud network bandwidth was set to 1 Mbps to simulate the close and distant proximity of mobile-edge and edge-cloud environments, respectively, based on earlier work [88,129,110,29,3]. The Computational simulations for resource-constrained tiers (i.e., mobile and edge) were also based on previous studies [19,23,58,96]. A previous study [95], utilized Docker containers on a server to simulate multiple tiers with limited resources within a practical Internet of Things (IoT) framework. This approach mirrors our methodology where we also simulated tiers with limited resources, specifically mobile and edge tiers.

In practical situations, there can be a range of hardware differences across various edge and mobile devices. These differences could potentially affect the broad applicability of our simulated environment.

[18] https://github.com/lutzroeder/netron

The process of simulating the effects of multiple variables is quite resource-intensive, requiring a significant amount of time and computational power to conduct a multitude of experiments, and therefore excluded from our study. While we recognize the significance of having varied deployment scenarios with different computational and network configurations for MEC tiers. Our specific experimental setup was strategically selected to concentrate on exploring a typical Edge AI setting comprising a resource-limited mobile device, an edge device with closer proximity and superior computational capacity compared to the mobile device, and a resource-rich cloud device subject to network limitations.

For Distillation, we used the teacher and student models coming from the same model family to make the knowledge transfer more straightforward and effective. Large teacher models were used to potentially transfer a more comprehensive set of insights to the student model. We used pre-trained models for them to provide a good starting point, aiding faster convergence during training. The default hyper-parameter values reported on the INC repository were adopted for white box operators (Distillation, QAT, Pruning) and black box operators (SPTQ) to maintain consistency with the reference implementation, ensuring results are interpretable within the INC framework. The choice of default hyper-parameters for the generation of white-box operators is quite common in previous work (Table 1), i.e., 56 out of 83 studies considered it. However, we do acknowledge that optimized values obtained via hyper-parameter tuning or analysis may exhibit different behaviors in response to accuracy/latency performance for the operators.

Internal Validity: We address potential historical influences on the inference latency results of deployment strategies by conducting all measurements in a consistent Edge AI environment with identical infrastructure. To mitigate variability and ensure uniformity, we developed automated scripts to execute inference experiments sequentially, one after another. Before each experiment, Docker containers were restarted to eliminate any lingering effects from prior runs. Unlike parallel inference scenarios, our experiments focused on sequential inference, processing one request at a time. This approach optimally utilizes resources for each deployment strategy, providing a more accurate reflection of their true inference performance, akin to the methodology employed in micro-benchmarks [128]. Notably, our study diverges from load testing [53], which typically assesses a system's capacity to handle multiple concurrent inference requests. The decision to prioritize sequential inference over parallel scenarios aims to avoid potential resource contention that might obscure the genuine impact of deployment strategies. Likewise, we have not delved into scalability considerations, such as how the quantity or complexity of models deployed concurrently would affect real-world scenarios. This aspect falls beyond the scope of our study since our micro-benchmarks are specifically focused on measuring individual model performance rather than broader system-level metrics.

The ONNX Run-time Inference Engine may exhibit latency delay on the initial input during inference experiments for deployment strategies due to a necessary warm-up inference. To address this bias, we implemented a trial inference experiment. For each deployment strategy, we conducted a trial experiment consisting of 100 sequential inference runs to establish a stable cache state. Subsequently, the final inference experiment, comprising 500 runs (100 input samples repeated 5 times), was conducted sequentially and repeatedly without intervening cool-down periods to assess the scalability of each deployment strategy. The selection of 100 input samples was based on a size filter to specifically analyze the impact of input data on inference latency.

External Validity: There is a potential threat associated with the manual selection of subject models, as this approach may not accurately represent the entire population. To diversify the inference tasks, we chose subject models from the Hugging Face and PyTorch Models store, focusing on both Image Classification and Text Classification tasks. The final set consisted of four models, two from each inference task. The majority of the previous studies (Table 1), focus on CV (79) and NLP (11) tasks for the operators during deployment in an Edge AI environment because they have a high influence on the amount of computations and data sent across the Edge AI environment. Therefore, the choice of CV and NLP domains for subject models and datasets is quite common. This external threat related to subject model selection can be addressed in future work by expanding the experiment to include other domain-specific subject models, such as Speech Models.

For simulating hardware and network configurations, we opted for Docker containers instead of actual devices. This choice provides flexibility in configuring network and hardware settings and is cost-effective compared to maintaining physical devices. Docker containers offer a way to create virtual environments that closely mimic real hardware behavior. The experiment used the latest tool and package versions on simulated devices, and to enhance generalization, future work could replicate the experiment on different hardware and network configurations. In the study, inference accuracy was independently computed on

multiple deployment tiers (Mobile, Edge, Cloud) for each operator (i.e., Identity, SPTQ, QAT, Pruned, Distilled, DSPTQ) to provide valuable insights into the model's generalizability across different hardware targets, specifically CPUs and GPUs. The ONNX models are designed to be hardware-agnostic which allows the ONNX models to achieve consistent accuracy across different deployment environments.

We applied the white box operators in Pytorch format due to INC's compatibility and integration limitations, and the resulting models were converted to ONNX format for uniformity in latency evaluation. The choice of INC as the framework for performing these white box operators is due to its readily available automated and streamlined training pipelines, as explained in Approach Section 3. One of the threats to the validity of the INC tool is the consideration of logical pruning instead of physical pruning for the subject models. Physical pruning is not yet supported for CV subject models in the INC tool and therefore, to do a fair and consistent analysis across the CV and textual subject models in our study, we limit the scope of pruning to logic-based approaches. For the QAT operator, the performance was measured in the Pytorch model due to performance issues with the ONNX model format as some of the PyTorch-specific QAT operations (i.e., fake quantization Ops) were not fully supported in the ONNX format. The selected ONNX framework as the format for the subject model representation because it serves as an open standard for model representation and interoperability by enabling the seamless exportation of models trained in different frameworks (such as PyTorch, TensorFlow, and MXNet). In terms of popularity, it is supported by major players like Microsoft [19], Facebook [20], and Nvidia [21]. We performed the inference of the operators using the ONNX Runtime Engine due to optimized deployment benefits, as suggested by previous studies [90,37].

7 Conclusion

Deploying white-box and black-box operators efficiently in an Edge AI setting introduces unique challenges for MLOps engineers and software practitioners. These operators require specific considerations for optimization in resource-constrained and network-constrained deployment scenarios. This paper aims to be an important stepping stone in the field of MLOps, in particular for the deployment of white-box operators, to evaluate the benefits and trade-offs of deployment strategies involving mappings of <operators, tiers>, by evaluating their performance with respect to metrics like Latency and Accuracy. While previous works focused on exploring and addressing individual white-box operators (i.e., Pruning, QAT, Distillation) and their combinations, our study extends on that by comparing them with the black-box operators (SPTQ, Partition) and their combinations (Distilled SPTQ, SPTQ Partition) in the specific context of an Edge AI setup of MEC tiers for both text and image classification subject models.

Among the single-tier and multi-tier deployment strategies, the MLOps engineers could prefer Edge and Cloud deployment for operators with higher (image) and smaller (text) input data size requirements, respectively when lower latency is a concern in deployment scenarios where the mobile tier has strict CPU/RAM requirements and the cloud tier has limited network bandwidth capacity. Among the non-hybrid operators deployed in resource-contained tiers, the Distilled operator could be the preferred choice over QAT, SPTQ, Pruned, and Identity operators, when faster latency is a requirement at small to medium accuracy loss. Furthermore, the DSPTQ hybrid operator could be a preferred choice over the non-hybrid operators (Identity, QAT, SPTQ, Pruned, Distilled) when faster latency is a requirement in edge at small to medium accuracy loss. For Distilled and DSPTQ operators, their deployment in resource-constrained tiers is more efficient in terms of latency than the MEIP and MESP strategies, respectively.

8 Conflict of Interests

All authors declare that they have no conflicts of interest.

[19] https://cloudblogs.microsoft.com/opensource/tag/onnx
[20] https://developers.facebook.com/blog/onnx/
[21] https://developer.nvidia.com/blog/tag/onnx/

9 Data Availability Statement

The data and code used during the current study are available at the below-mentioned GitHub repository: https://github.com/SAILResearch/wip-24-jaskirat-white-box-edge-operators.git.

References

1. Aghli, N., and Ribeiro, E. Combining weight pruning and knowledge distillation for cnn compression. In *Proceedings of the IEEE/CVF conference on computer vision and pattern recognition* (2021), pp. 3191–3198.
2. Ahn, J.-H., Simeone, O., and Kang, J. Wireless federated distillation for distributed edge learning with heterogeneous data. In *2019 IEEE 30th Annual International Symposium on Personal, Indoor and Mobile Radio Communications (PIMRC)* (2019), IEEE, pp. 1–6.
3. Andrés Ramiro, C., Fiandrino, C., Blanco Pizarro, A., Jiménez Mateo, P., Ludant, N., and Widmer, J. openleon: An end-to-end emulator from the edge data center to the mobile users. In *Proceedings of the 12th International Workshop on Wireless Network Testbeds, Experimental Evaluation & Characterization* (2018), pp. 19–27.
4. Assine, J. S., Valle, E., et al. Single-training collaborative object detectors adaptive to bandwidth and computation. *arXiv preprint arXiv:2105.00591* (2021).
5. Banitalebi-Dehkordi, A., Vedula, N., Pei, J., Xia, F., Wang, L., and Zhang, Y. Auto-split: A general framework of collaborative edge-cloud ai. In *Proceedings of the 27th ACM SIGKDD Conference on Knowledge Discovery & Data Mining* (2021), pp. 2543–2553.
6. Banner, R., Nahshan, Y., and Soudry, D. Post training 4-bit quantization of convolutional networks for rapid-deployment. *Advances in Neural Information Processing Systems 32* (2019).
7. Bhalgat, Y., Lee, J., Nagel, M., Blankevoort, T., and Kwak, N. Lsq+: Improving low-bit quantization through learnable offsets and better initialization. In *Proceedings of the IEEE/CVF Conference on Computer Vision and Pattern Recognition Workshops* (2020), pp. 696–697.
8. Bhattacharya, S., and Lane, N. D. Sparsification and separation of deep learning layers for constrained resource inference on wearables. In *Proceedings of the 14th ACM Conference on Embedded Network Sensor Systems CD-ROM* (2016), pp. 176–189.
9. Boo, Y., Shin, S., Choi, J., and Sung, W. Stochastic precision ensemble: self-knowledge distillation for quantized deep neural networks. In *Proceedings of the AAAI Conference on Artificial Intelligence* (2021), vol. 35, pp. 6794–6802.
10. Cai, Y., Yao, Z., Dong, Z., Gholami, A., Mahoney, M. W., and Keutzer, K. Zeroq: A novel zero shot quantization framework. In *Proceedings of the IEEE/CVF Conference on Computer Vision and Pattern Recognition* (2020), pp. 13169–13178.
11. Chandakkar, P. S., Li, Y., Ding, P. L. K., and Li, B. Strategies for re-training a pruned neural network in an edge computing paradigm. In *2017 IEEE International Conference on Edge Computing (EDGE)* (2017), IEEE, pp. 244–247.
12. Chang, J., Lu, Y., Xue, P., Xu, Y., and Wei, Z. Iterative clustering pruning for convolutional neural networks. *Knowledge-Based Systems 265* (2023), 110386.
13. Choi, J., Wang, Z., Venkataramani, S., Chuang, P. I.-J., Srinivasan, V., and Gopalakrishnan, K. Pact: Parameterized clipping activation for quantized neural networks. *arXiv preprint arXiv:1805.06085* (2018).
14. Choukroun, Y., Kravchik, E., Yang, F., and Kisilev, P. Low-bit quantization of neural networks for efficient inference. In *2019 IEEE/CVF International Conference on Computer Vision Workshop (ICCVW)* (2019), IEEE, pp. 3009–3018.
15. Cliff, N. Dominance statistics: Ordinal analyses to answer ordinal questions. *Psychological bulletin 114*, 3 (1993), 494.
16. Conover, W. J., and Iman, R. L. On multiple-comparisons procedures. *Los Alamos Sci. Lab. Tech. Rep. LA-7677-MS 1* (1979), 14.
17. Deng, S., Zhao, H., Fang, W., Yin, J., Dustdar, S., and Zomaya, A. Y. Edge intelligence: The confluence of edge computing and artificial intelligence. *IEEE Internet of Things Journal 7*, 8 (2020), 7457–7469.
18. Devlin, J., Chang, M.-W., Lee, K., and Toutanova, K. Bert: Pre-training of deep bidirectional transformers for language understanding. *arXiv preprint arXiv:1810.04805* (2018).
19. Dimolitsas, I., Spatharakis, D., Dechouniotis, D., Zafeiropoulos, A., and Papavassiliou, S. Multi-application hierarchical autoscaling for kubernetes edge clusters. In *2023 IEEE International Conference on Smart Computing (SMARTCOMP)* (2023), IEEE, pp. 291–296.
20. Dolan, B., and Brockett, C. Automatically constructing a corpus of sentential paraphrases. In *Third International Workshop on Paraphrasing (IWP2005)* (2005).
21. Dong, C., Hu, S., Chen, X., and Wen, W. Joint optimization with dnn partitioning and resource allocation in mobile edge computing. *IEEE Transactions on Network and Service Management 18*, 4 (2021), 3973–3986.
22. Dong, Z., Yao, Z., Gholami, A., Mahoney, M. W., and Keutzer, K. Hawq: Hessian aware quantization of neural networks with mixed-precision. In *Proceedings of the IEEE/CVF International Conference on Computer Vision* (2019), pp. 293–302.
23. Duan, Y., and Wu, J. Joint optimization of dnn partition and scheduling for mobile cloud computing. In *Proceedings of the 50th International Conference on Parallel Processing* (2021), pp. 1–10.
24. Dwivedi, A. K., Mallawaarachchi, I., and Alvarado, L. A. Analysis of small sample size studies using nonparametric bootstrap test with pooled resampling method. *Statistics in medicine 36*, 14 (2017), 2187–2205.
25. Esser, S. K., McKinstry, J. L., Bablani, D., Appuswamy, R., and Modha, D. S. Learned step size quantization. *arXiv preprint arXiv:1902.08153* (2019).

26. Fan, A., Stock, P., Graham, B., Grave, E., Gribonval, R., Jegou, H., and Joulin, A. Training with quantization noise for extreme model compression. *arXiv preprint arXiv:2004.07320* (2020).
27. Fang, B., Zeng, X., and Zhang, M. Nestdnn: Resource-aware multi-tenant on-device deep learning for continuous mobile vision. In *Proceedings of the 24th Annual International Conference on Mobile Computing and Networking* (2018), pp. 115–127.
28. Fang, J., Shafiee, A., Abdel-Aziz, H., Thorsley, D., Georgiadis, G., and Hassoun, J. H. Post-training piecewise linear quantization for deep neural networks. In *Computer Vision–ECCV 2020: 16th European Conference, Glasgow, UK, August 23–28, 2020, Proceedings, Part II 16* (2020), Springer, pp. 69–86.
29. Fiandrino, C., Pizarro, A. B., Mateo, P. J., Ramiro, C. A., Ludant, N., and Widmer, J. openleon: An end-to-end emulation platform from the edge data center to the mobile user. *Computer Communications 148* (2019), 17–26.
30. Garg, S., Jain, A., Lou, J., and Nahmias, M. Confounding tradeoffs for neural network quantization. *arXiv preprint arXiv:2102.06366* (2021).
31. Garg, S., Lou, J., Jain, A., Guo, Z., Shastri, B. J., and Nahmias, M. Dynamic precision analog computing for neural networks. *IEEE Journal of Selected Topics in Quantum Electronics 29*, 2: Optical Computing (2022), 1–12.
32. Gholami, A., Kim, S., Dong, Z., Yao, Z., Mahoney, M. W., and Keutzer, K. A survey of quantization methods for efficient neural network inference. In *Low-Power Computer Vision*. Chapman and Hall/CRC, 2022, pp. 291–326.
33. Gou, J., Yu, B., Maybank, S. J., and Tao, D. Knowledge distillation: A survey. *International Journal of Computer Vision 129* (2021), 1789–1819.
34. Guadagnoli, E., and Velicer, W. F. Relation of sample size to the stability of component patterns. *Psychological bulletin 103*, 2 (1988), 265.
35. Gupta, S., Agrawal, A., Gopalakrishnan, K., and Narayanan, P. Deep learning with limited numerical precision. In *International conference on machine learning* (2015), PMLR, pp. 1737–1746.
36. Guskin, S., Wasserblat, M., Wang, C., and Shen, H. Quala-minilm: a quantized length adaptive minilm. *arXiv preprint arXiv:2210.17114* (2022).
37. Hampau, R. M., Kaptein, M., Van Emden, R., Rost, T., and Malavolta, I. An empirical study on the performance and energy consumption of ai containerization strategies for computer-vision tasks on the edge. In *Proceedings of the International Conference on Evaluation and Assessment in Software Engineering 2022* (2022), pp. 50–59.
38. Han, S., Kang, J., Mao, H., Hu, Y., Li, X., Li, Y., Xie, D., Luo, H., Yao, S., Wang, Y., et al. Ese: Efficient speech recognition engine with sparse lstm on fpga. In *Proceedings of the 2017 ACM/SIGDA International Symposium on Field-Programmable Gate Arrays* (2017), pp. 75–84.
39. Han, S., Mao, H., and Dally, W. J. Deep compression: Compressing deep neural networks with pruning, trained quantization and huffman coding. *arXiv preprint arXiv:1510.00149* (2015).
40. Han, S., Pool, J., Tran, J., and Dally, W. Learning both weights and connections for efficient neural network. *Advances in neural information processing systems 28* (2015).
41. Hawks, B., Duarte, J., Fraser, N. J., Pappalardo, A., Tran, N., and Umuroglu, Y. Ps and qs: Quantization-aware pruning for efficient low latency neural network inference. *Frontiers in Artificial Intelligence 4* (2021), 676564.
42. He, X., and Cheng, J. Learning compression from limited unlabeled data. In *Proceedings of the European Conference on Computer Vision (ECCV)* (2018), pp. 752–769.
43. Hess, M. R., and Kromrey, J. D. Robust confidence intervals for effect sizes: A comparative study of cohen'sd and cliff's delta under non-normality and heterogeneous variances. In *annual meeting of the American Educational Research Association* (2004), vol. 1, Citeseer.
44. Hinton, G., Vinyals, O., and Dean, J. Distilling the knowledge in a neural network. *arXiv preprint arXiv:1503.02531* (2015).
45. Holm, S. A simple sequentially rejective multiple test procedure. *Scandinavian journal of statistics* (1979), 65–70.
46. Hu, P., Peng, X., Zhu, H., Aly, M. M. S., and Lin, J. Opq: Compressing deep neural networks with one-shot pruning-quantization. In *Proceedings of the AAAI Conference on Artificial Intelligence* (2021), vol. 35, pp. 7780–7788.
47. Hubara, I., Nahshan, Y., Hanani, Y., Banner, R., and Soudry, D. Improving post training neural quantization: Layer-wise calibration and integer programming. *arXiv preprint arXiv:2006.10518* (2020).
48. Idelbayev, Y., and Carreira-Perpiñán, M. Á. An empirical comparison of quantization, pruning and low-rank neural network compression using the lc toolkit. In *2021 International Joint Conference on Neural Networks (IJCNN)* (2021), IEEE, pp. 1–8.
49. Jacob, B., Kligys, S., Chen, B., Zhu, M., Tang, M., Howard, A., Adam, H., and Kalenichenko, D. Quantization and training of neural networks for efficient integer-arithmetic-only inference. In *Proceedings of the IEEE conference on computer vision and pattern recognition* (2018), pp. 2704–2713.
50. Jain, S., Gural, A., Wu, M., and Dick, C. Trained quantization thresholds for accurate and efficient fixed-point inference of deep neural networks. *Proceedings of Machine Learning and Systems 2* (2020), 112–128.
51. Jankowski, M., Gündüz, D., and Mikolajczyk, K. Joint device-edge inference over wireless links with pruning. In *2020 IEEE 21st international workshop on signal processing advances in wireless communications (SPAWC)* (2020), IEEE, pp. 1–5.
52. Jiang, Y., Wang, S., Valls, V., Ko, B. J., Lee, W.-H., Leung, K. K., and Tassiulas, L. Model pruning enables efficient federated learning on edge devices. *IEEE Transactions on Neural Networks and Learning Systems* (2022).
53. Jiang, Z. M., and Hassan, A. E. A survey on load testing of large-scale software systems. *IEEE Transactions on Software Engineering 41*, 11 (2015), 1091–1118.
54. Jin, J., Liang, C., Wu, T., Zou, L., and Gan, Z. Kdlsq-bert: A quantized bert combining knowledge distillation with learned step size quantization. *arXiv preprint arXiv:2101.05938* (2021).
55. Kim, J. Quantization robust pruning with knowledge distillation. *IEEE Access 11* (2023), 26419–26426.
56. Kim, J., Bhalgat, Y., Lee, J., Patel, C., and Kwak, N. Qkd: Quantization-aware knowledge distillation. *arXiv preprint arXiv:1911.12491* (2019).
57. Kim, J., Chang, S., and Kwak, N. Pqk: model compression via pruning, quantization, and knowledge distillation. *arXiv preprint arXiv:2106.14681* (2021).

58. Künas, C. A. Optimizing machine learning models training in the cloud.
59. Kuzmin, A., Nagel, M., Van Baalen, M., Behboodi, A., and Blankevoort, T. Pruning vs quantization: Which is better? *Advances in Neural Information Processing Systems 36* (2024).
60. Lee, J. H., Ha, S., Choi, S., Lee, W.-J., and Lee, S. Quantization for rapid deployment of deep neural networks. *arXiv preprint arXiv:1810.05488* (2018).
61. Lee, N., Ajanthan, T., and Torr, P. H. Snip: Single-shot network pruning based on connection sensitivity. *arXiv preprint arXiv:1810.02340* (2018).
62. Li, E., Zhou, Z., and Chen, X. Edge intelligence: On-demand deep learning model co-inference with device-edge synergy. In *Proceedings of the 2018 Workshop on Mobile Edge Communications* (2018), pp. 31–36.
63. Li, G., Liu, L., Wang, X., Dong, X., Zhao, P., and Feng, X. Auto-tuning neural network quantization framework for collaborative inference between the cloud and edge. In *Artificial Neural Networks and Machine Learning–ICANN 2018: 27th International Conference on Artificial Neural Networks, Rhodes, Greece, October 4-7, 2018, Proceedings, Part I 27* (2018), Springer, pp. 402–411.
64. Li, G., Ma, X., Wang, X., Yue, H., Li, J., Liu, L., Feng, X., and Xue, J. Optimizing deep neural networks on intelligent edge accelerators via flexible-rate filter pruning. *Journal of Systems Architecture 124* (2022), 102431.
65. Li, H., Zhang, H., Qi, X., Yang, R., and Huang, G. Improved techniques for training adaptive deep networks. In *Proceedings of the IEEE/CVF international conference on computer vision* (2019), pp. 1891–1900.
66. Li, Y., Gong, R., Tan, X., Yang, Y., Hu, P., Zhang, Q., Yu, F., Wang, W., and Gu, S. Brecq: Pushing the limit of post-training quantization by block reconstruction. *arXiv preprint arXiv:2102.05426* (2021).
67. Lin, D., Talathi, S., and Annapureddy, S. Fixed point quantization of deep convolutional networks. In *International conference on machine learning* (2016), PMLR, pp. 2849–2858.
68. Liu, S., Lin, Y., Zhou, Z., Nan, K., Liu, H., and Du, J. On-demand deep model compression for mobile devices: A usage-driven model selection framework. In *Proceedings of the 16th annual international conference on mobile systems, applications, and services* (2018), pp. 389–400.
69. Liu, W., Zhou, P., Zhao, Z., Wang, Z., Deng, H., and Ju, Q. Fastbert: a self-distilling bert with adaptive inference time. *arXiv preprint arXiv:2004.02178* (2020).
70. Liu, Y., Ott, M., Goyal, N., Du, J., Joshi, M., Chen, D., Levy, O., Lewis, M., Zettlemoyer, L., and Stoyanov, V. Roberta: A robustly optimized bert pretraining approach. *arXiv preprint arXiv:1907.11692* (2019).
71. Louizos, C., Reisser, M., Blankevoort, T., Gavves, E., and Welling, M. Relaxed quantization for discretized neural networks. *arXiv preprint arXiv:1810.01875* (2018).
72. Lu, D., and Weng, Q. A survey of image classification methods and techniques for improving classification performance. *International journal of Remote sensing 28*, 5 (2007), 823–870.
73. Matsubara, Y., Baidya, S., Callegaro, D., Levorato, M., and Singh, S. Distilled split deep neural networks for edge-assisted real-time systems. In *Proceedings of the 2019 Workshop on Hot Topics in Video Analytics and Intelligent Edges* (2019), pp. 21–26.
74. Matsubara, Y., Callegaro, D., Singh, S., Levorato, M., and Restuccia, F. Bottlefit: Learning compressed representations in deep neural networks for effective and efficient split computing. In *2022 IEEE 23rd International Symposium on a World of Wireless, Mobile and Multimedia Networks (WoWMoM)* (2022), IEEE, pp. 337–346.
75. Matsubara, Y., and Levorato, M. Split computing for complex object detectors: Challenges and preliminary results. In *Proceedings of the 4th International Workshop on Embedded and Mobile Deep Learning* (2020), pp. 7–12.
76. Matsubara, Y., and Levorato, M. Neural compression and filtering for edge-assisted real-time object detection in challenged networks. In *2020 25th International Conference on Pattern Recognition (ICPR)* (2021), IEEE, pp. 2272–2279.
77. Matsubara, Y., Yang, R., Levorato, M., and Mandt, S. Sc2 benchmark: Supervised compression for split computing. *arXiv e-prints* (2022), arXiv–2203.
78. Matsubara, Y., Yang, R., Levorato, M., and Mandt, S. Supervised compression for resource-constrained edge computing systems. In *Proceedings of the IEEE/CVF Winter Conference on Applications of Computer Vision* (2022), pp. 2685–2695.
79. Meller, E., Finkelstein, A., Almog, U., and Grobman, M. Same, same but different: Recovering neural network quantization error through weight factorization. In *International Conference on Machine Learning* (2019), PMLR, pp. 4486–4495.
80. Merkel, D. Docker: Lightweight linux containers for consistent development and deployment. *Linux J. 2014*, 239 (mar 2014).
81. Mohammed, T., Joe-Wong, C., Babbar, R., and Di Francesco, M. Distributed inference acceleration with adaptive dnn partitioning and offloading. In *IEEE INFOCOM 2020-IEEE Conference on Computer Communications* (2020), IEEE, pp. 854–863.
82. Movva, R., Lei, J., Longpre, S., Gupta, A., and DuBois, C. Combining compressions for multiplicative size scaling on natural language tasks. *arXiv preprint arXiv:2208.09684* (2022).
83. Murshed, M. S., Murphy, C., Hou, D., Khan, N., Ananthanarayanan, G., and Hussain, F. Machine learning at the network edge: A survey. *ACM Computing Surveys (CSUR) 54*, 8 (2021), 1–37.
84. Na, J., Zhang, H., Lian, J., and Zhang, B. Genetic algorithm-based online-partitioning branchynet for accelerating edge inference. *Sensors 23*, 3 (2023), 1500.
85. Nagel, M., Amjad, R. A., Van Baalen, M., Louizos, C., and Blankevoort, T. Up or down? adaptive rounding for post-training quantization. In *International Conference on Machine Learning* (2020), PMLR, pp. 7197–7206.
86. Nagel, M., Baalen, M. v., Blankevoort, T., and Welling, M. Data-free quantization through weight equalization and bias correction. In *Proceedings of the IEEE/CVF International Conference on Computer Vision* (2019), pp. 1325–1334.
87. Nagel, M., Fournarakis, M., Bondarenko, Y., and Blankevoort, T. Overcoming oscillations in quantization-aware training. In *International Conference on Machine Learning* (2022), PMLR, pp. 16318–16330.
88. Nan, Y., Jiang, S., and Li, M. Large-scale video analytics with cloud–edge collaborative continuous learning. *ACM Transactions on Sensor Networks 20*, 1 (2023), 1–23.

89. Neshatpour, K., Homayoun, H., and Sasan, A. Icnn: The iterative convolutional neural network. *ACM Transactions on Embedded Computing Systems (TECS) 18*, 6 (2019), 1–27.
90. Openja, M., Nikanjam, A., Yahmed, A. H., Khomh, F., Ming, Z., et al. An empirical study of challenges in converting deep learning models. *arXiv preprint arXiv:2206.14322* (2022).
91. Ostertagova, E., Ostertag, O., and Kováč, J. Methodology and application of the kruskal-wallis test. In *Applied mechanics and materials* (2014), vol. 611, Trans Tech Publ, pp. 115–120.
92. Phuong, M., and Lampert, C. H. Distillation-based training for multi-exit architectures. In *Proceedings of the IEEE/CVF international conference on computer vision* (2019), pp. 1355–1364.
93. Pistellato, M., Bergamasco, F., Bigaglia, G., Gasparetto, A., Albarelli, A., Boschetti, M., and Passerone, R. Quantization-aware nn layers with high-throughput fpga implementation for edge ai. *Sensors 23*, 10 (2023), 4667.
94. Portabales, A. R., and Nores, M. L. Dockemu: Extension of a scalable network simulation framework based on docker and ns3 to cover iot scenarios. In *SIMULTECH* (2018), pp. 175–182.
95. Portabales, A. R., and Nores, M. L. Dockemu: An iot simulation framework based on linux containers and the ns-3 network simulator—application to coap iot scenarios. In *Simulation and Modeling Methodologies, Technologies and Applications: 8th International Conference, SIMULTECH 2018, Porto, Portugal, July 29-31, 2018, Revised Selected Papers* (2020), Springer, pp. 54–82.
96. Qian, J., Li, J., Ma, R., Lin, L., and Guan, H. Lg-ram: Load-aware global resource affinity management for virtualized multicore systems. *Journal of Systems Architecture 98* (2019), 114–125.
97. Reagen, B., Whatmough, P., Adolf, R., Rama, S., Lee, H., Lee, S. K., Hernández-Lobato, J. M., Wei, G.-Y., and Brooks, D. Minerva: Enabling low-power, highly-accurate deep neural network accelerators. *ACM SIGARCH Computer Architecture News 44*, 3 (2016), 267–278.
98. Russakovsky, O., Deng, J., Su, H., Krause, J., Satheesh, S., Ma, S., Huang, Z., Karpathy, A., Khosla, A., Bernstein, M., Berg, A. C., and Fei-Fei, L. ImageNet Large Scale Visual Recognition Challenge. *International Journal of Computer Vision (IJCV) 115*, 3 (2015), 211–252.
99. Sakr, C., Dai, S., Venkatesan, R., Zimmer, B., Dally, W., and Khailany, B. Optimal clipping and magnitude-aware differentiation for improved quantization-aware training. In *International Conference on Machine Learning* (2022), PMLR, pp. 19123–19138.
100. Sbai, M., Saputra, M. R. U., Trigoni, N., and Markham, A. Cut, distil and encode (cde): Split cloud-edge deep inference. In *2021 18th Annual IEEE International Conference on Sensing, Communication, and Networking (SECON)* (2021), IEEE, pp. 1–9.
101. Sepahvand, M., Abdali-Mohammadi, F., and Taherkordi, A. An adaptive teacher–student learning algorithm with decomposed knowledge distillation for on-edge intelligence. *Engineering Applications of Artificial Intelligence 117* (2023), 105560.
102. Sharma, R., Biookaghazadeh, S., and Zhao, M. Are existing knowledge transfer techniques effective for deep learning on edge devices? In *Proceedings of the 27th International Symposium on High-Performance Parallel and Distributed Computing* (2018), pp. 15–16.
103. Shen, H., Mellempudi, N., He, X., Gao, Q., Wang, C., and Wang, M. Efficient post-training quantization with fp8 formats. *arXiv preprint arXiv:2309.14592* (2023).
104. Shen, H., Zafrir, O., Dong, B., Meng, H., Ye, X., Wang, Z., Ding, Y., Chang, H., Boudoukh, G., and Wasserblat, M. Fast distilbert on cpus. *arXiv preprint arXiv:2211.07715* (2022).
105. Shen, M., Liang, F., Gong, R., Li, Y., Li, C., Lin, C., Yu, F., Yan, J., and Ouyang, W. Once quantization-aware training: High performance extremely low-bit architecture search. In *Proceedings of the IEEE/CVF International Conference on Computer Vision* (2021), pp. 5340–5349.
106. Shin, S., Boo, Y., and Sung, W. Knowledge distillation for optimization of quantized deep neural networks. In *2020 IEEE Workshop on Signal Processing Systems (SiPS)* (2020), IEEE, pp. 1–6.
107. Shomron, G., Gabbay, F., Kurzum, S., and Weiser, U. Post-training sparsity-aware quantization. *Advances in Neural Information Processing Systems 34* (2021), 17737–17748.
108. Singh, J., Adams, B., and Hassan, A. E. On the impact of black-box deployment strategies for edge ai on latency and model performance, 2024.
109. Singh, S., Sharma, K., Karna, B. K., and Raj, P. A new bert-inspired knowledge distillation approach toward compressed ai models for edge devices. In *International Conference on Security, Privacy and Data Analytics* (2022), Springer, pp. 105–117.
110. Suryavansh, S., Bothra, C., Chiang, M., Peng, C., and Bagchi, S. Tango of edge and cloud execution for reliability. In *Proceedings of the 4th Workshop on Middleware for Edge Clouds & Cloudlets* (2019), pp. 10–15.
111. Tailor, S. A., Fernandez-Marques, J., and Lane, N. D. Degree-quant: Quantization-aware training for graph neural networks. *arXiv preprint arXiv:2008.05000* (2020).
112. Tang, J., Shivanna, R., Zhao, Z., Lin, D., Singh, A., Chi, E. H., and Jain, S. Understanding and improving knowledge distillation. *arXiv preprint arXiv:2002.03532* (2020).
113. Tung, F., and Mori, G. Deep neural network compression by in-parallel pruning-quantization. *IEEE transactions on pattern analysis and machine intelligence 42*, 3 (2018), 568–579.
114. Turc, I., Chang, M.-W., Lee, K., and Toutanova, K. Well-read students learn better: On the importance of pre-training compact models. *arXiv preprint arXiv:1908.08962* (2019).
115. Uhlich, S., Mauch, L., Cardinaux, F., Yoshiyama, K., Garcia, J. A., Tiedemann, S., Kemp, T., and Nakamura, A. Mixed precision dnns: All you need is a good parametrization. *arXiv preprint arXiv:1905.11452* (2019).
116. Van Baalen, M., Louizos, C., Nagel, M., Amjad, R. A., Wang, Y., Blankevoort, T., and Welling, M. Bayesian bits: Unifying quantization and pruning. *Advances in neural information processing systems 33* (2020), 5741–5752.
117. Wang, A., Singh, A., Michael, J., Hill, F., Levy, O., and Bowman, S. R. Glue: A multi-task benchmark and analysis platform for natural language understanding. *arXiv preprint arXiv:1804.07461* (2018).
118. Wang, X., Han, Y., Leung, V. C., Niyato, D., Yan, X., and Chen, X. Convergence of edge computing and deep learning: A comprehensive survey. *IEEE Communications Surveys & Tutorials 22*, 2 (2020), 869–904.

119. Wohlin, C., Runeson, P., Höst, M., Ohlsson, M. C., Regnell, B., and Wesslén, A. *Experimentation in software engineering*. Springer Science & Business Media, 2012.
120. Xie, S., Girshick, R., Dollár, P., Tu, Z., and He, K. Aggregated residual transformations for deep neural networks, 2017.
121. Xu, M., Qian, F., Zhu, M., Huang, F., Pushp, S., and Liu, X. Deepwear: Adaptive local offloading for on-wearable deep learning. *IEEE Transactions on Mobile Computing 19*, 2 (2019), 314–330.
122. Yang, C., and Liu, H. Channel pruning based on convolutional neural network sensitivity. *Neurocomputing 507* (2022), 97–106.
123. Yang, H., Gui, S., Zhu, Y., and Liu, J. Automatic neural network compression by sparsity-quantization joint learning: A constrained optimization-based approach. In *Proceedings of the IEEE/CVF Conference on Computer Vision and Pattern Recognition* (2020), pp. 2178–2188.
124. Yang, T.-J., Chen, Y.-H., and Sze, V. Designing energy-efficient convolutional neural networks using energy-aware pruning. In *Proceedings of the IEEE conference on computer vision and pattern recognition* (2017), pp. 5687–5695.
125. Yang, X., Chen, D., Qi, Q., Wang, J., Sun, H., Liao, J., and Guo, S. Adaptive dnn surgery for selfish inference acceleration with on-demand edge resource. *arXiv preprint arXiv:2306.12185* (2023).
126. Zafrir, O., Larey, A., Boudoukh, G., Shen, H., and Wasserblat, M. Prune once for all: Sparse pre-trained language models. *arXiv preprint arXiv:2111.05754* (2021).
127. Zagoruyko, S., and Komodakis, N. Wide residual networks, 2017.
128. Zhang, L. L., Han, S., Wei, J., Zheng, N., Cao, T., Yang, Y., and Liu, Y. Nn-meter: Towards accurate latency prediction of deep-learning model inference on diverse edge devices. In *Proceedings of the 19th Annual International Conference on Mobile Systems, Applications, and Services* (2021), pp. 81–93.
129. Zhang, X., Mounesan, M., and Debroy, S. Effect-dnn: Energy-efficient edge framework for real-time dnn inference. In *2023 IEEE 24th International Symposium on a World of Wireless, Mobile and Multimedia Networks (WoWMoM)* (2023), IEEE, pp. 10–20.
130. Zhao, R., Hu, Y., Dotzel, J., De Sa, C., and Zhang, Z. Improving neural network quantization without retraining using outlier channel splitting. In *International conference on machine learning* (2019), PMLR, pp. 7543–7552.
131. Zhao, X., Xu, R., and Guo, X. Post-training quantization or quantization-aware training? that is the question. In *2023 China Semiconductor Technology International Conference (CSTIC)* (2023), IEEE, pp. 1–3.
132. Zhou, Q., Guo, S., Qu, Z., Guo, J., Xu, Z., Zhang, J., Guo, T., Luo, B., and Zhou, J. Octo:{INT8} training with loss-aware compensation and backward quantization for tiny on-device learning. In *2021 USENIX Annual Technical Conference (USENIX ATC 21)* (2021), pp. 177–191.
133. Zhou, S., Wu, Y., Ni, Z., Zhou, X., Wen, H., and Zou, Y. Dorefa-net: Training low bitwidth convolutional neural networks with low bitwidth gradients. *arXiv preprint arXiv:1606.06160* (2016).
134. Zhou, Z., Chen, X., Li, E., Zeng, L., Luo, K., and Zhang, J. Edge intelligence: Paving the last mile of artificial intelligence with edge computing. *Proceedings of the IEEE 107*, 8 (2019), 1738–1762.

Appendices

Appendix A Graphical Illustrations of Manual algorithms used for the black-box operators

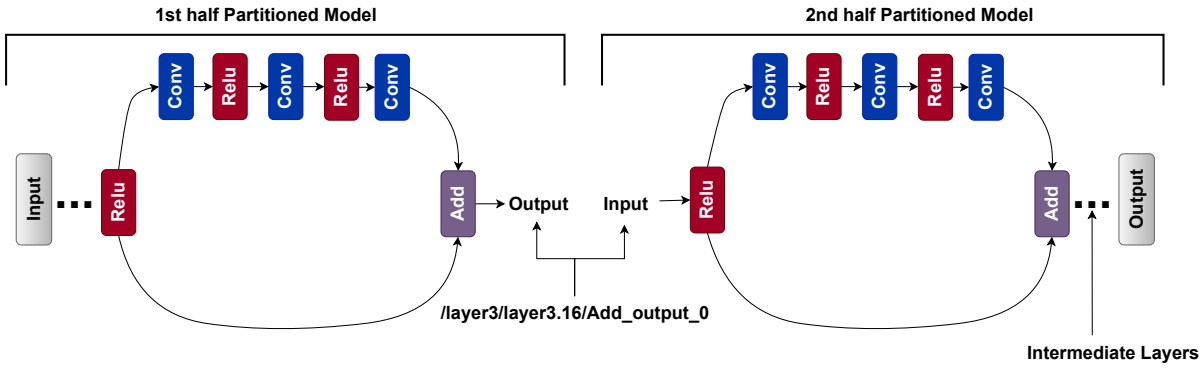

Fig. 11: Graphical Illustration of Partitioning for ResNet and ResNext (Copied with permission from [108])

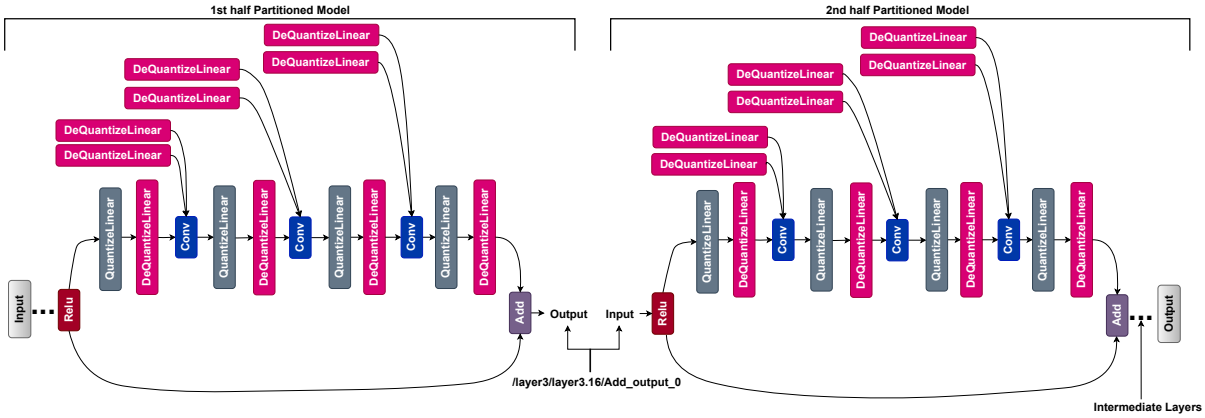

Fig. 12: Graphical Illustration of Quantized Partitioning for ResNet and ResNext (Copied with permission from [108])

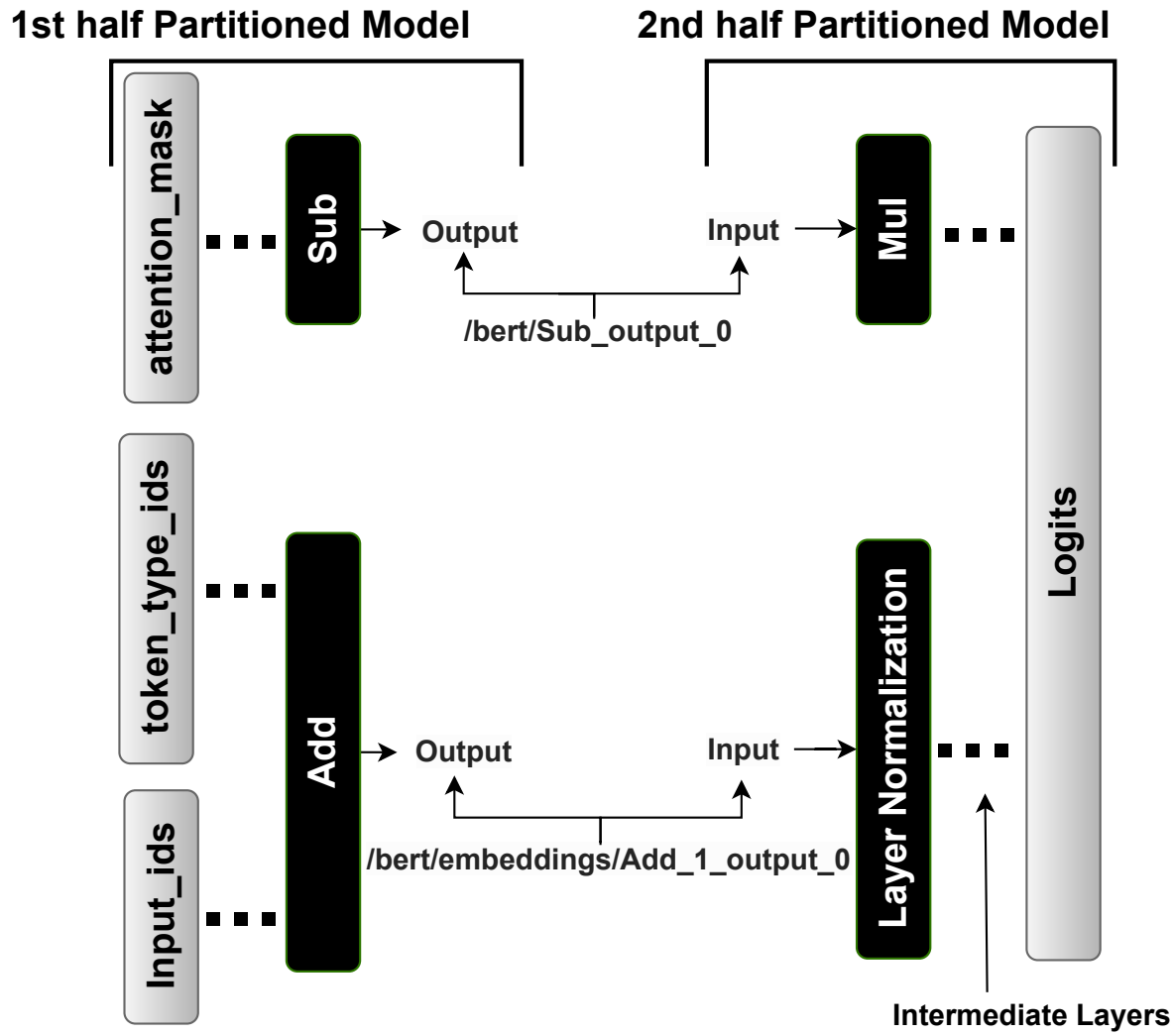

Fig. 13: Graphical Illustration of Partitioning for Bert

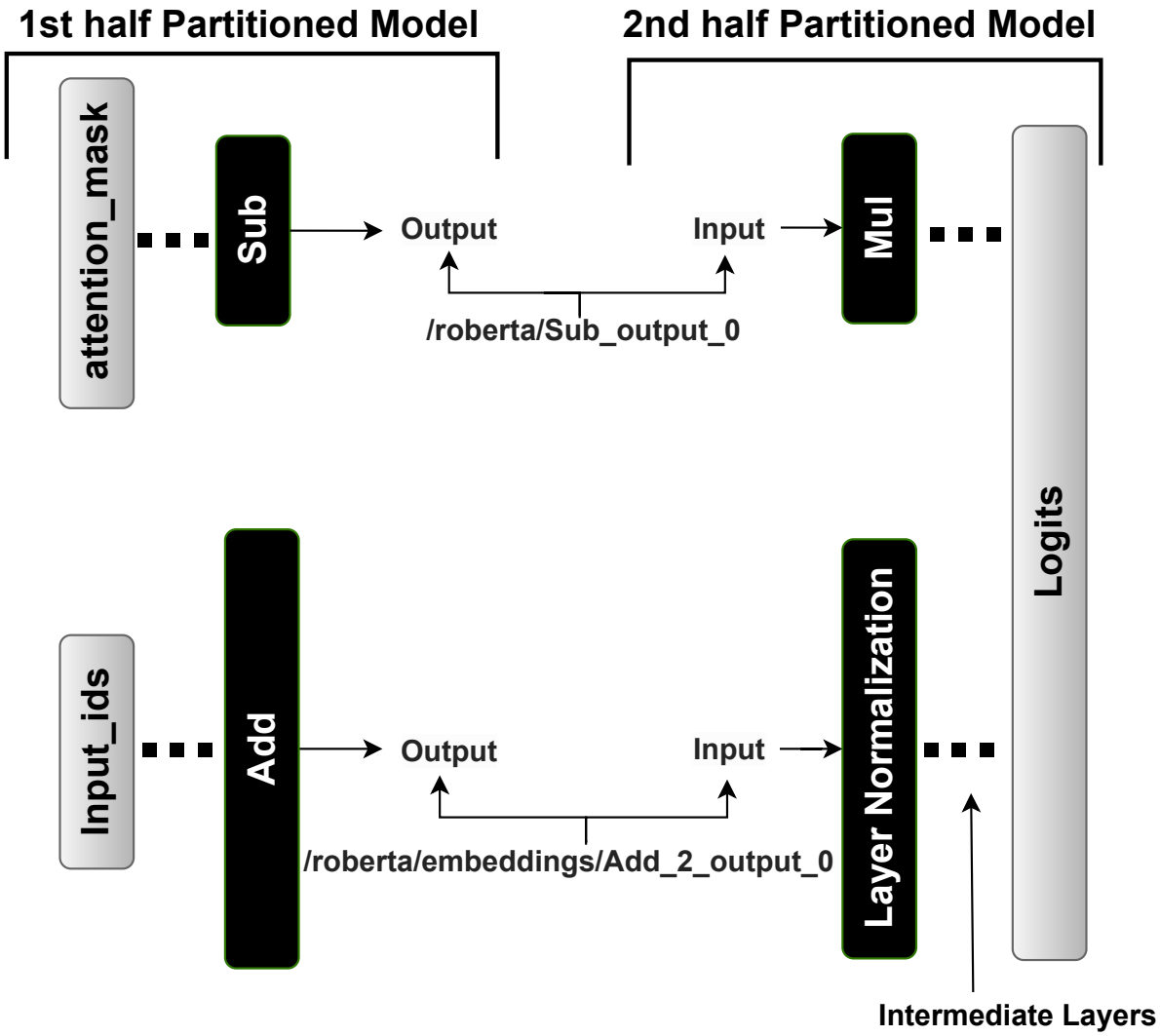

Fig. 14: Graphical Illustration of Partitioning for Roberta

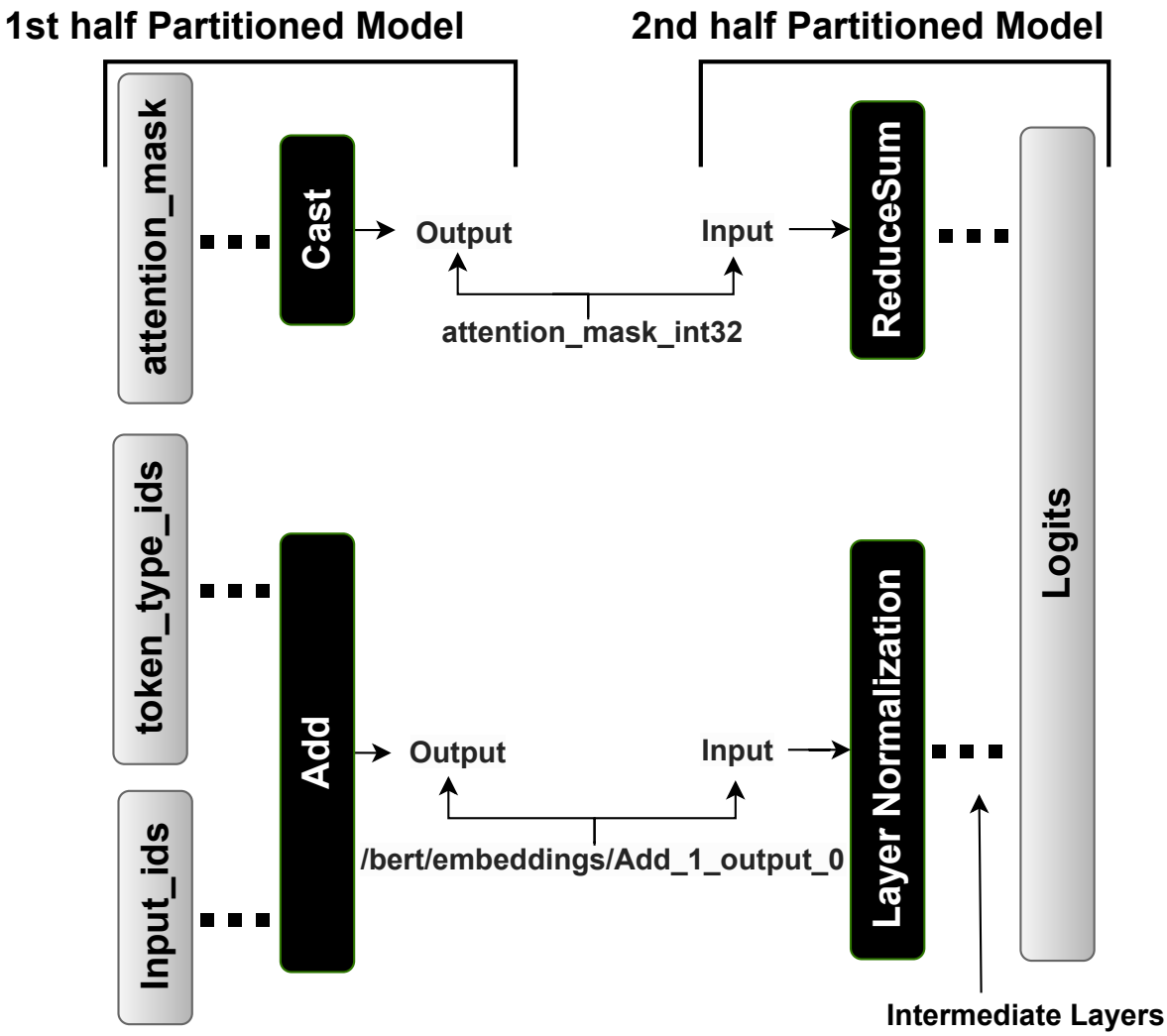

Fig. 15: Graphical Illustration of Quantized Partitioning for Bert

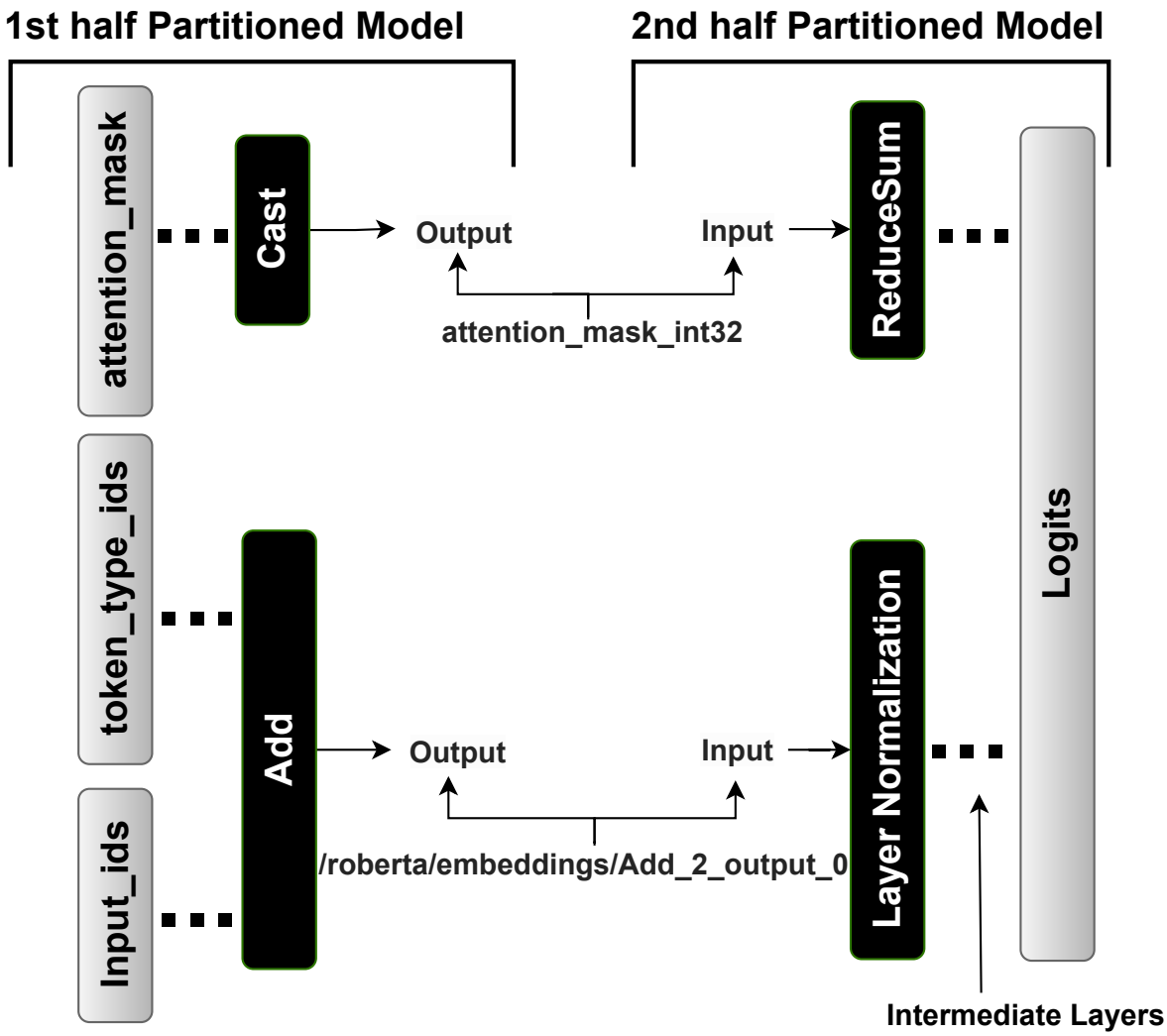

Fig. 16: Graphical Illustration of Quantized Partitioning for Roberta